NASA TECHNICAL NOTE

NASA TN D-3147

NASA TN D-3147

A GUIDANCE SCHEME FOR LUNAR DESCENT BASED ON LINEAR PERTURBATION THEORY

by Kenneth C. White and Phillips J. Tunnell

Ames Research Center
Moffett Field, Calif.

NATIONAL AERONAUTICS AND SPACE ADMINISTRATION • WASHINGTON, D. C. • DECEMBER 1965

NASA TN D-3147

A GUIDANCE SCHEME FOR LUNAR DESCENT BASED ON LINEAR PERTURBATION THEORY

By Kenneth C. White and Phillips J. Tunnell

Ames Research Center
Moffett Field, Calif.

NATIONAL AERONAUTICS AND SPACE ADMINISTRATION

For sale by the Clearinghouse for Federal Scientific and Technical Information
Springfield, Virginia 22151 – Price $2.00

A GUIDANCE SCHEME FOR LUNAR DESCENT BASED ON LINEAR PERTURBATION THEORY

By Kenneth C. White and Phillips J. Tunnell
Ames Research Center

SUMMARY

A three-dimensional guidance scheme for descending from lunar orbit to a hovering position was developed and analyzed. The scheme is based on the linear theory of perturbations about a nominal reference trajectory and uses thrust acceleration and thrust orientation angles as variables in the control equations. It allows the preselection of a lunar landing site from a wide range of initial conditions and permits guidance within the rigid constraints proposed for LEM. The specific control equations are fully developed in the report. Guidance capability, the effect on guidance capability of reducing the target size, and fuel consumption are considered in detail. An analog computer was used for the investigation and the basic results were checked by means of a digital computer program.

INTRODUCTION

The powered descent from lunar orbit to a hovering position near the lunar surface is critical for various reasons. The vehicle will be required to reach a preselected hovering point, and restraints on position and velocity will be very stringent. The amount of propellant required will influence the earth launch requirements and the payload delivered to the lunar surface. Excessive fuel consumption during the powered descent would reduce hovering time, thus limiting the time allowed for selecting a desirable landing site. These are some of the major problems of a lunar descent.

Various guidance schemes have been investigated for the powered lunar descent (e.g., refs. 1-6). A two-dimensional guidance scheme for lunar descent was developed in reference 1. It was based on linear perturbation theory and two types of reference trajectories, the gravity-turn and constant pitch-rate maneuvers. The purpose of this report is to extend the two-dimensional gravity-turn study of reference 1 to a full three-dimensional analysis. In addition, a different variable, thrust acceleration rather than thrust, will be used in the guidance equations because it is more readily measured. The control equations thus differ from those of reference 1 and new two-dimensional guidance results are presented. The specific equations necessary for three-dimensional guidance are developed in the appendix. Detailed fuel consumption data are presented to show the efficiency of the guidance system.

The effect on guidance capability of reducing the target area and of initial errors in vehicle flight-path angle is also shown.

The performance of the guidance system was investigated by simulating the system and mechanizing the equations of motion on an analog computer. The basic results were checked using a digital computer program.

The authors are indebted to Dr. Richard Rosenbaum of Lockheed Missiles and Space Company for pointing out the advantages of using thrust acceleration as a control variable.

NOTATION

A_T	thrust acceleration, g
F_x^u	linear theory gain for the x state variable used to determine the magnitude of the control variable, u, dimensions of u/x
g_e	earth surface gravity
h	altitude above lunar surface, m
I_{sp}	specific impulse, sec
m	mass, kg
r	$r_m + h$, km
r_m	radius of moon, km
T	thrust, N
V	total velocity, m/sec
X	$r_m\Psi$, range, km
X_{TG}	range to go, km
Y	$r_m\Lambda$, lateral range, km
γ	flight-path angle (sketch (b)), deg
$\delta( )$	difference between actual and reference value, $( )_a - ( )_r$
ζ	heading angle (sketch (b)), rad
θ	thrust angle (sketch (c)), rad
Λ	lateral range angle (sketch (a)), rad
λ_x^u	$\left(\frac{\partial u}{\partial x}\right)$ adjoint variable

μ product of universal gravitational constant and mass of planet, m^3/sec^2

Ψ range angle (sketch (a)), rad

ψ thrust angle (sketch (c)), rad

$(\dot{})$ derivative with respect to time

$( )'$ derivative with respect to velocity

Subscripts

a actual

f final

i initial

j,k summing indices

r reference

LUNAR LANDING APPROACH

Figure 1 is a schematic diagram of a lunar landing maneuver. It is assumed that a manned space vehicle enters a 160 km (100 statute miles) circular orbit about the moon from a direct earth-moon trajectory. The vehicle then performs a transfer maneuver, which places it in an elliptical lunar orbit with a perilune of 22,900 m (75,000 ft) and makes a powered descent from perilune.

The Hohmann transfer maneuver is assumed here; however, any transfer maneuver that will place the vehicle in a lunar orbit with a perilune of 22,900 m (75,000 ft) could be used. The guidance scheme in this report is developed for the descent from perilune and does not include the transfer maneuver.

REFERENCE TRAJECTORY

The nominal or reference trajectory chosen as a basis for developing the guidance system is the same constant-thrust gravity-turn descent trajectory that was considered in reference 1. It begins at perilune of the elliptic transfer orbit and terminates at the hover altitude of 300 m (1,000 ft). The initial altitude is 22,900 m (75,000 ft) and the trajectory traverses approximately 300 km (190 statute miles) of lunar surface. Pertinent quantities of the reference trajectory are shown in figure 2.

The gravity-turn reference trajectory was chosen primarily because it is convenient and requires less than 5 percent more characteristic velocity than an optimum trajectory beginning at the same perilune altitude (ref. 7).

PERFORMANCE CRITERIA

In this investigation the target area was assumed to be 300 km (190 miles) from the reference trajectory perilune. The dimensions of the target area are the same as those used in reference 1, that is, altitude, ±150 m (±500 ft), and range, ±1,500 m (±5,000 ft). An additional dimension of ±1,500 m (±5,000 ft) is assumed for crossrange. The center of the target area is at the hover altitude of 300 m (1,000 ft). Performance capabilities, presented elsewhere in this report, are based on the ability of the vehicle to reach this target area with less than 3 mps (10 fps) vertical velocity and less than 3 mps (10 fps) total velocity. Performance capabilities based on target areas that are 1/2 and 1/4 of the aforementioned target area are also presented and compared with the capabilities based on the nominal target area. The comparison gives some indication of the effect of target area dimensions on the guidance system capability.

No performance criteria were selected for fuel consumption; fuel consumption data for the trajectories investigated are presented simply to indicate the fuel necessary to attain the guidance capabilities.

INITIAL CONDITIONS

In this investigation initial perilune altitudes were considered up to ±9,200 m (±35,000 ft) from the reference and initial ranges, 240 to 900 km (150 to 560 miles) from the target. The reference trajectory range is approximately 300 km (190 statute miles). Initial lateral displacements up to 160 km (100 statute miles) outside the plane of the reference trajectory were also considered. The expected errors in altitude, range, and crossrange for a LEM mission are considerably smaller than the spread of initial conditions considered here.

GUIDANCE EQUATION

The concept of guidance about a nominal or reference trajectory is based on perturbation theory, that is, the analysis of conditions in a limited neighborhood of a nominal trajectory. The basic linear perturbation theory guidance equation is developed in reference 1. To control altitude above the lunar surface, h, range, X, and lateral range, Y, at the hover point, the quantities, thrust acceleration, A_T, thrust pitch angle, θ, and thrust yaw angle, ψ, are varied. Thrust acceleration rather than thrust is the control variable because it is more easily measured, the number of terms in the guidance equations are reduced, and deviations in thrust and mass from their

nominal values are accounted for by one readily available measurement. Thus, fewer guidance gains are required and less onboard computer storage is required.

The specific guidance equations used in this investigation are developed in the appendix. They are:

$$\left.\begin{aligned} A_T(V) &= A_{T_r}(V) + F_h^{A_T}(V)\delta h + F_x^{A_T}(V)\delta x + F_\gamma^{A_T}(V)\delta\gamma \\ \theta(V) &= \theta_r(V) + F_h^{\theta}(V)\delta h + F_x^{\theta}(V)\delta x + F_\gamma^{\theta}(V)\delta\gamma \\ \psi(V) &= \psi_r(V) + F_y^{\psi}(V)\delta Y + F_\zeta^{\psi}(V)\delta\zeta \end{aligned}\right\} \qquad (1)$$

where total velocity, V, is the independent variable, $\delta(\ )$ is the difference between the actual and reference value, $(\ )_a - (\ )_r$, and F are the guidance gains defined in the appendix.

Total velocity, V, rather than time, was chosen as the independent variable to reduce the number of terms in equations (1) by one, thus simplifying the equations and reducing information storage requirements.

A flow diagram of the guidance system operation is given in figure 3 in terms of a general guidance equation. Note that the reference state variables, reference control variables, and guidance gains are stored as functions of the independent variable velocity. Control increments are computed on the basis of differences between the actual trajectory and the reference trajectory at a given velocity.

The guidance equations with thrust acceleration, A_T, used as a control variable allow the effect of perturbations in thrust and mass from their nominal values to be combined into a single term ΔA_T.

GUIDANCE GAINS

The calculated linear theory guidance gains associated with equations (1) are shown in figure 4. The performance capability was investigated by simulating the guidance system on an analog computer. Because of the limited storage capacity of this computer, the guidance gains were stored for 17 velocity points with linear interpolation between points. To insure accuracy in storing the gains within the scaling and storage restrictions of the analog equipment, the gains were limited as indicated by the dashed lines of figure 4.

An important result of reference 1 was that the guidance capability could be greatly increased by weighting the guidance gains empirically. In the

present study the gains in figure 4 were increased and decreased individually, and it was found that increasing the gain F_h^θ by a factor of 2.5 and F_Λ^B by a factor of 1.5 substantially improved the guidance capability. It should be emphasized that these factors are not optimum in any way. They are merely two of the more effective values of the guidance gains discovered by increasing and decreasing the gains individually. The adjusted gains were limited at the same value of velocity as were the gains in figure 4, and no attempt was made to adjust more than one gain at a time. There are various methods of adjusting the gains; one simple method would be to change the value of velocity at which the gains were limited. Conceivably there are other combinations of adjustments which would similarly increase capability but no attempt was made to find any optimum set of guidance gains. The intent is simply to show that the guidance capability can be improved in a manner similar to that demonstrated in reference 1.

An IBM 7094 digital computer program was used to check the analog computer results. Many more than 17 points were used, making it possible to ascertain the validity of the simpler storage of the analog computer. Since the digital and analog results compared quite well, the analog storage is considered valid.

An attempt was made to further simplify the guidance gains by approximating each gain shown in figure 4 with a single straight line. Several different combinations of single straight line approximations were investigated but in each case the guidance capability was greatly reduced in comparison with the linear theory capability. This gives some indication of the importance of the shape of the guidance gain curves.

VEHICLE CHARACTERISTICS AND EQUATIONS OF MOTION

If the vehicle is assumed to be a point mass, and the moon to be spherical and nonrotating, the resulting equations of motion are:

$$\dot{h} = V \sin \gamma$$

$$\dot{\gamma} = \frac{T \sin \theta \cos \psi}{mV} + \frac{V}{r} \cos \gamma - \frac{1}{V} \frac{\mu}{r^2} \cos \gamma$$

$$\dot{V} = \frac{T \cos \theta \cos \psi}{m} - \frac{\mu}{r^2} \sin \gamma$$

$$\dot{\zeta} = \frac{T \sin \psi}{mV \cos \gamma} - \frac{V}{r} \tan \Lambda \cos \gamma \cos \zeta$$

$$\dot{Y} = r_m \dot{\Lambda} = \frac{r_m}{r} V \cos \gamma \sin \zeta$$

$$\dot{X} = r_m \dot{\Psi} = \frac{r_m}{r} \frac{V \cos \gamma \cos \zeta}{\cos \Lambda}$$

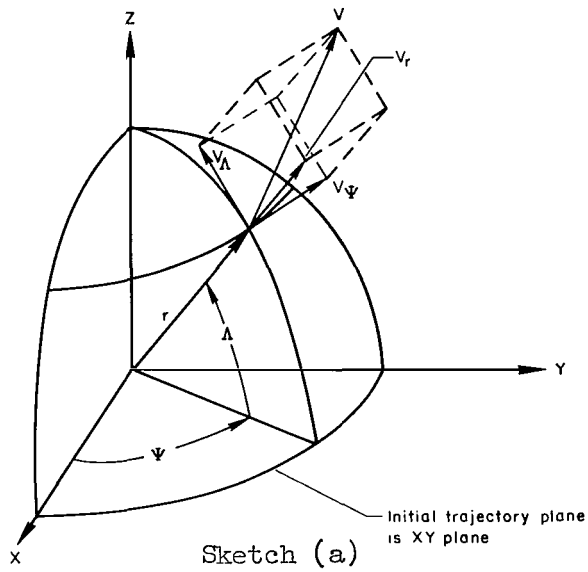

Sketch (a)

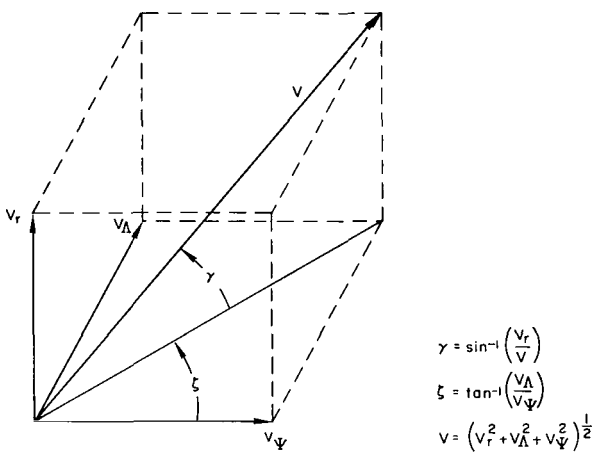

Sketch (b)

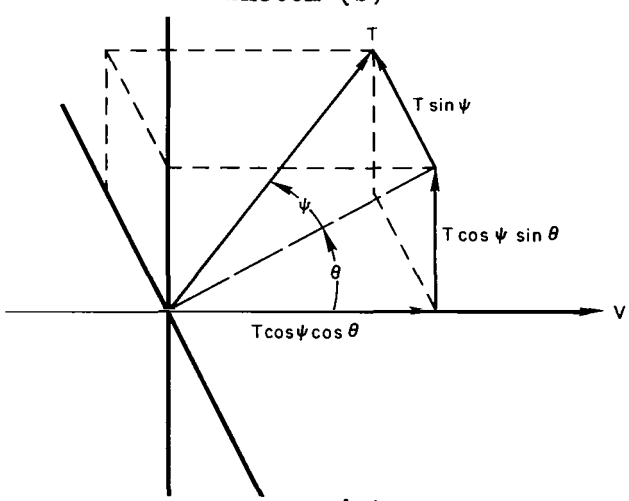

Sketch (c)

The mass rate is given by $\dot{m} = m_i - \int(T/g_e I_{sp})dt$, where I_{sp} equals 425 seconds. The geometry for the equations of motion is shown in sketches (a), (b), and (c). Sketch (a) presents the axis system for the trajectory equations. The coordinate system is centered at the center of the moon. Sketch (b) defines flight-path angle γ and heading angle ζ. Thrust angle orientation is shown in sketch (c). Thrust pitch angle θ is the angle between the velocity vector and the projection of the thrust vector in the vertical plane. The thrust yaw angle ψ is the angle between the thrust vector and the vertical plane.

The vehicle is assumed to have a gimballed, variable-thrust rocket engine. No throttle ratio was imposed but the minimum thrust was limited to 1.11×10^4 N (2,500 lb) which was one-tenth the reference thrust. The guidance system actually required a maximum thrust of 156,000 N (35,000 lb) to achieve the full three-dimensional capability shown elsewhere in this report. A maximum thrust of 142,000 N (32,000 lb) was required for the two-dimensional capability. Two-dimensional capability for ranges longer than the reference range required maximum thrust to be less than 111,000 N (25,000 lb).

RESULTS

Two-Dimensional Guidance Capability

The two-dimensional guidance capability of the guidance system when the descent maneuver is initiated at perilune of an elliptic Hohmann trajectory is illustrated in figure 5(a). The capability is presented in terms of the initial altitude and range limits from which it is possible to meet the altitude and range constraints of the aforementioned target area. Initial

values of altitude and velocity correspond to the Hohmann trajectory with perilune at that point. Since the descent was always initiated at perilune, the vehicle's initial flight-path angle and vertical velocity are zero.

The smaller capability indicated by the shaded area was obtained from the linear theory guidance gains of figure 4. The increased capability indicated by the boundaries labeled "limits of investigation," which include the shaded area, was obtained by increasing the gain F_h^θ by a factor of 2.5.

The heavy black lines of figure 5(a) indicate limits of capability defined by the investigation. The target constraints which were exceeded are also indicated.

For the guidance capability in figure 5(a) numerous initial points were considered at three different perilune altitudes; the reference value and the two altitudes corresponding to the altitude limits of investigation, namely, 12,200 m (40,000 ft) and 33,500 m (110,000 ft). Initial range-to-go values were varied at intervals of approximately 40 km (25 statute miles) across the region of capability. A brief check was made of the results for trajectories whose perilune altitude was intermediate to the three discussed above and also of trajectories whose initial range to go was intermediate to the intervals of 40 km. Results for these intermediate trajectories correlated well with the basic data. The consistency of results for this large amount of data indicates that guidance to the target area could be achieved from any point within the region of capability.

Figure 5(b) is a comparison of the guidance capability using the linear theory gains with capability as presented in reference 1 using linear theory gains. As indicated, the capability is generally greater for the guidance scheme presented in this report. The improved capability is a result of taking into account vehicle mass perturbations in the development of the guidance equations. The guidance results from using empirically adjusted gains are not compared directly as it would be extremely difficult to determine which set of guidance equations would yield greater extended capability. The intent here is to verify that the capability can be extended in the manner shown in reference 1.

Figure 5(c) compares the guidance capability for the nominal target with that for two targets, the dimensions of which are one-half and one-fourth of the nominal dimensions. As indicated, the capability is substantially reduced when guiding to a smaller target. The data in figure 5(c) are for the linear theory gains.

In figure 5(d) the same comparison is made for capability using the empirically adjusted gains. In this case the capability is not altered by target size.

The two-dimensional guidance capability of the system when the descent is initiated at a point other than perilune is presented in figure 6 in terms of the initial altitude and range limits from which it is possible to meet the altitude and range constraints of the target area. Since the descent is not initiated at perilune, initial flight-path angle and vertical velocity are not zero. For the purposes of this phase of the investigation it was assumed

that the Hohmann transfer is always initiated at the same apolune point 160 km (100 statute miles) above the lunar surface. Therefore, initial conditions are determined by the Hohmann trajectory passing through that point. Values of flight-path angle along three of the Hohmann trajectories considered are given in figure 7. Initial flight-path angles ranging from -0.8° to 0.1° were considered. The corresponding vertical velocities ranged from -23 m/sec to 6 m/sec (-75 ft/sec to 20 ft/sec).

The smaller capability indicated by the shaded area resulted from using the calculated gains of figure 4 and the increased capability indicated by the boundaries labeled "limits of the investigation," which include the shaded area, was again obtained by increasing the gain F_h^{θ} by a factor of 2.5. Again the heavy black lines indicate defined limits of capability and the constraints which define the limits are also indicated.

The guidance capability presented in figure 6 was determined in a manner similar to that used for figure 5(a). Descents were initiated at numerous points along three trajectories whose perilunes were located at the reference range from the target. The perilune altitudes were 12,200 m (40,000 ft), 22,900 m (75,000 ft), and 30,500 m (100,000 ft). The interval between values of initial range to go was again approximately 40 km (25 statute miles). Again the consistency of the data indicates the vehicle can reach the target area from any point within the region of capability.

In both figure 5(a) and figure 6, the only limit of capability when the gain 2.5 F_h^{θ} is used is for shorter ranged trajectories than the reference. This limit was defined by failure to meet range constraints. Elsewhere the capability extends to the limits of the investigation.

Three-dimensional guidance capability.- The results discussed thus far are for two-dimensional trajectories. Now consider trajectories which have an initial lateral displacement out of the plane of the reference trajectory. Descent is initiated at perilune. The initial conditions of figures 8(a), 8(b), and 8(c) are identical to those of figure 5(a) with an added initial lateral displacement. Figures 8(a), 8(b), and 8(c) present the lateral guidance capability for three different perilune altitudes in terms of the initial lateral displacement and range limits from which it is possible to guide to the specified target area. The smaller capability, indicated by the dashed lines, was obtained using the values of F_y^{ψ} and F_{ζ}^{ψ} given in figure 4. The wider capability for each altitude, indicated by the solid lines, was obtained by increasing F_y^{ψ} by a factor of 1.5. This factor was one of the more effective values discovered by increasing and decreasing F_y^{ψ} and F_{ζ}^{ψ} separately. Other combinations of gain adjustments might give equally good increased capability but, again, no attempt was made to obtain an optimum set of gains. In all three-dimensional work, the gain 2.5 F_h^{θ} was also used.

The constraints which were exceeded in defining the limits of capability are indicated in figure 8.

A comparison of figures 8(a), 8(b), and 8(c) shows that lateral capability is greater at lower altitudes for short ranged trajectories and greater at higher altitudes for longer ranged trajectories when the gain 1.5 F_y^{ψ} is used. When the linear values of F_y^{ψ} is used, the capability is generally larger for higher altitudes. The maximum lateral capability is 160 km (100 statute miles) initial displacement. This is the lateral capability for a descent whose perilune is at 33,500 m (110,000 ft) altitude located 900 km (560 statute miles) from the target. In general, the system has a large lateral capability with linear theory gains which may be increased with adjusted gains. It will be pointed out in the next section that fuel consumption is greatly increased for trajectories having initial lateral displacements. This increased fuel consumption may limit the useful lateral capability.

An important conclusion of the study of lateral range guidance is that the addition of the third dimension to be controlled does not reduce in any way the two-dimensional guidance capability.

FUEL REQUIREMENTS

Figures 9(a), 9(b), and 9(c) present the additional characteristic velocity, ΔV_c, required for the lateral range capabilities with the adjusted gain 1.5 F_y^{ψ} in figure 8. Additional velocity, ΔV_c, is defined as V_c of the actual trajectory minus V_c of the reference trajectory, $\Delta V_c = V_{c_a} - V_{c_r}$, where $V_c = g_e I_{sp} \ln(m_i/m_f)$. The curves shown represent ΔV_c as a function of initial lateral range, Y_i, and initial range to go, X_{TG_i}. The figures indicate that the guidance system requires little ΔV_c if the vehicle is not required to change orbital plane. The maximum ΔV_c required for the two-dimensional trajectories of figure 5 is only 21 m (70 ft) per second. The system can cope with initial lateral displacements of 24 to 40 km (15 to 25 statute miles) with only a small additional ΔV_c. However, as initial lateral displacement increases, the characteristic velocity, which is a measure of fuel consumption, becomes an important consideration and may limit the lateral capability. The large increases in ΔV_c with initial lateral displacements result from the necessity to change the plane of the trajectory.

CONCLUDING REMARKS

A three-dimensional guidance scheme for the descent from lunar orbit to hover has been investigated. The guidance scheme was developed by applying linear perturbation theory to a single nominal or reference trajectory. It is shown that the scheme has guidance capability beyond that required for lunar descent of the type proposed for the LEM. Thrust acceleration, A_t, a readily measured quantity, and thrust orientation angles are used as control variables. With this scheme a hover point near the lunar surface can be preselected from a wide range of initial conditions; empirical weighting of the computed guidance coefficients would compensate for initial ranges of 240 to 900 km (150 to 560 statute miles) from the target, from altitudes of 12,200 to 33,500 m (40,000 to 110,000 ft), and initial lateral displacements up to 160 km (100 statute miles) outside the plane of the reference trajectory.

Range and altitude guidance is accomplished with only a nominal increase in fuel consumption but lateral displacements require more.

An important result of this study is that the addition of a third dimension to the guidance does not reduce the two-dimensional capability.

Empirically adjusted gains permit guidance to a much smaller target area with only a small decrease in guidance capability.

Since only a single nominal trajectory is used, little onboard computer storage capacity is required.

Ames Research Center
National Aeronautics and Space Administration
Moffett Field, Calif., Sept. 7, 1965

APPENDIX

DEVELOPMENT OF SPECIFIC CONTROL EQUATION

It is desired to develop a terminal guidance system based on the application of linear perturbation theory to the reference trajectory. The linear perturbation equations which describe the motion of a body near a nominal trajectory are the total differentials of the equations of motion. They are of the form:

$$d\dot{p} = \frac{\partial \dot{p}}{\partial h}\delta h + \frac{\partial \dot{p}}{\partial x}\delta x + \frac{\partial \dot{p}}{\partial \gamma}\delta\gamma + \frac{\partial \dot{p}}{\partial V}\delta V + \frac{\partial \dot{p}}{\partial y}\delta y + \frac{\partial \dot{p}}{\partial \zeta}\delta\zeta + \frac{\partial \dot{p}}{\partial A_T}\delta A_T + \frac{\partial \dot{p}}{\partial \theta}\delta\theta + \frac{\partial \dot{p}}{\partial \psi}\delta\psi \tag{A1}$$

or

$$\delta\dot{p} = A_{i1}\delta h + A_{i2}\delta X + A_{i3}\delta\gamma + A_{i4}\delta V + A_{i5}\delta y + A_{i6}\delta\zeta + b_{i1}\delta A_T + b_{i2}\delta\theta + b_{i3}\delta\psi \tag{A2}$$

where

$$p = h,\ x,\ \gamma,\ V,\ Y,\ \zeta$$

and

$$i = 1,\ 2,\ 3,\ 4,\ 5,\ 6$$

The control variables are thrust acceleration, A_T, thrust pitch angle, θ, and thrust yaw angle, ψ. The use of thrust acceleration as a control variable simplifies the control equations by allowing the effect of perturbations in mass and thrust to be combined into a single term, ΔA_T.

Total velocity, V, is the independent variable in the control equations. The equations of motion are written thus:

$$\left.\begin{aligned} \dot{p} &= \frac{dp}{dt} = \frac{dp}{dV}\frac{dV}{dt} = p'\dot{V} \\ \text{or} \qquad p' &= \frac{\dot{p}}{\dot{V}} \end{aligned}\right\} \tag{A3}$$

where $p = h,\ X,\ \gamma,\ \Lambda,\ \zeta$ and the prime refers to differentiation with respect to total velocity, V.

The linear perturbation equations now become:

$$dp' = \frac{\partial p'}{\partial h}\delta h + \frac{\partial p'}{\partial x}\delta X + \frac{\partial p'}{\partial \gamma}\delta\gamma + \frac{\partial p'}{\partial Y}\delta Y + \frac{\partial p'}{\partial \zeta}\delta\zeta + \frac{\partial p'}{\partial A_T}\delta A_T + \frac{\partial p'}{\partial \theta}\delta\theta + \frac{\partial p'}{\partial \psi}\delta\psi \tag{A4}$$

or

$$\delta p' = A_{k1}\delta h + A_{k2}\delta X + A_{k3}\delta\gamma + A_{k4}\delta Y + A_{k5}\delta\zeta + B_{k1}\delta A_T + B_{K2}\delta\theta + B_{K3}\delta\Psi \tag{A5}$$

where

$$p = h,\ X,\ \gamma,\ Y,\ \zeta$$

and

$$k = 1,\ 2,\ 3,\ 4,\ 5$$

The partial derivatives are evaluated for the constant-thrust gravity-turn reference trajectory. By definition, $\theta = 180^\circ$ on the reference trajectory and, since a planar trajectory is assumed, $\Lambda = \zeta = \Psi = 0$. The nonzero coefficients of equation (A5) are found to be:

$$A_{11} = \frac{\partial h'}{\partial h} = \frac{-\dot{h}}{\dot{V}^2}\frac{2\mu}{r^3}\sin\gamma$$

$$A_{13} = \frac{\partial h'}{\partial \gamma} = \frac{V\cos\gamma}{\dot{V}} + \frac{\mu}{r^2}\cos\gamma\frac{\dot{h}}{\dot{V}^2}$$

$$A_{21} = \frac{\partial X'}{\partial h} = \frac{-r_m V\cos\gamma}{r^2\dot{V}} - \frac{2\mu}{r^3}\sin\gamma\frac{\dot{X}}{\dot{V}^2}$$

$$A_{23} = \frac{\partial X'}{\partial \gamma} = \frac{-r_m V\sin\gamma}{r\dot{V}} + \frac{\mu}{r^2}\cos\gamma\frac{\dot{X}}{\dot{V}^2}$$

$$A_{31} = \frac{\partial \gamma'}{\partial h} = \frac{\dfrac{-V\cos\gamma}{r^2} + \dfrac{2\mu}{Vr^3}\cos\gamma}{\dot{V}} - \frac{\dot{\gamma}\dfrac{2\mu}{r^2}\cos\gamma}{\dot{V}^2}$$

$$A_{33} = \frac{\partial \gamma'}{\partial \gamma} = \frac{\dfrac{-V}{r}\sin\gamma + \dfrac{1}{V}\dfrac{\mu}{r^2}\sin\gamma}{\dot{V}} + \frac{\dfrac{\mu}{r^2}\cos\gamma\dot{\gamma}}{\dot{V}^2}$$

$$A_{45} = \frac{\partial Y'}{\partial \zeta} = \frac{r_m}{r}\frac{V\cos\gamma}{\dot{V}}$$

$$A_{54} = \frac{\partial \zeta'}{\partial Y} = \frac{-V\cos\gamma}{r\dot{V}}$$

$$B_{11} = \frac{\partial h'}{\partial A_T} = \frac{\dot{h}}{\dot{V}^2}$$

$$B_{21} = \frac{\partial X'}{\partial A_T} = \frac{\dot{X}}{\dot{V}^2}$$

$$B_{31} = \frac{\partial \gamma'}{\partial A_T} = \frac{\dot{\gamma}}{\dot{V}^2}$$

$$B_{32} = \frac{\partial \gamma'}{\partial \theta} = \frac{-T}{mV\dot{V}}$$

$$B_{53} = \frac{\partial \zeta'}{\partial \psi} = \frac{T}{mV \cos \gamma \dot{V}}$$

In matrix form the linear perturbation equations are:

$$\begin{bmatrix} \delta h' \\ \delta X' \\ \delta \gamma' \\ \delta Y' \\ \delta \zeta' \end{bmatrix} = \begin{bmatrix} A_{11} & 0 & A_{13} & 0 & 0 \\ A_{21} & 0 & A_{23} & 0 & 0 \\ A_{31} & 0 & A_{33} & 0 & 0 \\ 0 & 0 & 0 & 0 & A_{45} \\ 0 & 0 & 0 & A_{54} & 0 \end{bmatrix} \begin{bmatrix} \delta h \\ \delta X \\ \delta \gamma \\ \delta Y \\ \delta \zeta \end{bmatrix} + \begin{bmatrix} B_{11} & 0 & 0 \\ B_{21} & 0 & 0 \\ B_{31} & B_{32} & 0 \\ 0 & 0 & 0 \\ 0 & 0 & B_{53} \end{bmatrix} \begin{bmatrix} \delta A_T \\ \delta \theta \\ \delta \psi \end{bmatrix} \quad (A6)$$

They are linear differential equations with variable coefficients. It should be noted that the last two equations are uncoupled from the others, indicating that, to first order, the heading angle ζ and lateral displacement Y are independent of range, altitude, and flight-path angle. This is only true for a planar reference trajectory.

Values of δh, δX, $\delta \gamma$, δY, and $\delta \zeta$ at the final velocity, V_f, can be determined, if their values are known at some initial velocity, V_i, by setting $\delta A_T = \delta \theta = \delta \psi = 0$. The effect of a control variable on the final values of the state variables can be found by solving the perturbation equations with all other variables initially equal to zero.

This method of computing control increments must be repeated for every new V_i because of the variable coefficient equations. It becomes extremely cumbersome to calculate control increments at every point along the trajectory. This may be avoided if the method of adjoint functions is used (see ref. 8). One solution of the equations adjoint to the linear perturbation equations yields all the required information.

In matrix form the equations adjoint to the linear perturbation equations (A6) are:

$$\begin{bmatrix} \lambda_h' \\ \lambda_X' \\ \lambda_\gamma' \\ \lambda_Y' \\ \lambda_\zeta' \end{bmatrix} = - \begin{bmatrix} A_{11} & A_{21} & A_{31} & 0 & 0 \\ 0 & 0 & 0 & 0 & 0 \\ A_{13} & A_{23} & A_{33} & 0 & 0 \\ 0 & 0 & 0 & 0 & A_{54} \\ 0 & 0 & 0 & A_{45} & 0 \end{bmatrix} \begin{bmatrix} \lambda_h \\ \lambda_X \\ \lambda_\gamma \\ \lambda_Y \\ \lambda_\zeta \end{bmatrix} \quad (A7)$$

Equations (A6) may be written

$$X_k' - \sum_{j=1}^{5} a_{kj}X_j = \sum_{j=1}^{3} b_{kj}\rho_j \tag{A8}$$

and equations (A7) may be written

$$\lambda_k' + \sum_{j=1}^{5} a_{jk}\lambda_j = 0 \tag{A9}$$

Now multiply (A8) by λ_k and (A9) by X_k; then add and sum over k:

$$\sum_{k=1}^{5} (\lambda_k X_k' + X_k\lambda_k') + \sum_{j=1}^{5}\sum_{k=1}^{5} (X_k a_{jk}\lambda_j - X_j a_{kj}\lambda_k) = \sum_{k=1}^{5}\sum_{j=1}^{3} \lambda_k b_{kj}\rho_j \tag{A10}$$

The second term in (A10) is zero since j and k are summing indices over the same range. Therefore (A10) becomes

$$\sum_{k=1}^{5} (\lambda_k X_k' + X_k\lambda_k') = \sum_{k=1}^{5}\sum_{j=1}^{3} \lambda_k b_{kj}\rho_j \tag{A11}$$

The left-hand side is a perfect differential so write (A11)

$$\frac{d}{dV}\sum_{k=1}^{5} (\lambda_k X_k) = \sum_{k=1}^{5}\sum_{j=1}^{3} \lambda_k b_{kj}\rho_j$$

Integrating (A11) from $V = V_1$ to $V = V_f$ gives

$$\sum_{k=1}^{5} \lambda_k(V_f)X_k(V_f) = \sum_{k=1}^{5} \lambda_k(V_1)X_k(V_1) + \int_{V_1}^{V_f} \sum_{k=1}^{5}\sum_{j=1}^{3} \lambda_k(V)b_{kj}(V)\rho_j(V)dV \tag{A12}$$

Equation (A12), Bliss' fundamental formula, is the basic equation for control about a reference trajectory (see ref. 9).

Substituting values from (A7) and (A8) into (A12) gives the following equation:

$$[\lambda_h\delta h + \lambda_X\delta X + \lambda_\gamma\delta\gamma + \lambda_Y\delta Y + \lambda_\zeta\delta\zeta]_{V=V_f}$$
$$= [\lambda_h\delta h + \lambda_X\delta X + \lambda_\gamma\delta\gamma + \lambda_Y\delta Y + \lambda_\zeta\delta\zeta]_{V=V_1}$$
$$+ \int_{V_1}^{V_f} (b_{32}\lambda_\gamma\delta\theta + b_{41}\lambda_Y\delta A_T + b_{63}\lambda_\zeta\delta\psi)dV \tag{A13}$$

To control the final altitude, h, range, X, and lateral displacement, Y, we must solve equation (A13) for the final errors δh_f, δX_f, and δY_f at $V = V_f$. Note that the left-hand side of (A13) equals δh_f (if $\lambda_h = 1$ and all other λ's are zero). Solving (A13) in this manner for δh_f, δX_f, and δY_f yields the following expressions:

$$\left.\begin{aligned}
\delta h_f &= \left[\lambda_h^h \delta h + \lambda_\gamma^h \delta\gamma\right]_{V=V_1} + \int_{V_1}^{V_f} (B_{11}\lambda_h^h + B_{31}\lambda_\gamma^h)\delta A_T \, dV + \int_{V_1}^{V_f} B_{32}\lambda_\gamma^h \delta\theta \, dV \\
\delta X_f &= \left[\lambda_h^X \delta h + \delta X + \lambda_\gamma^X \delta\gamma\right]_{V=V_1} + \int_{V_1}^{V_f} (B_{11}\lambda_h^X + B_{21} + B_{31}\lambda_\gamma^X) dV + \int_{V_1}^{V_f} B_{32}\lambda_\gamma^X \delta\theta \, dV \\
\delta Y_f &= \left[\lambda_Y^Y \delta Y + \lambda_\zeta^Y \delta\zeta\right]_{V=V_1} + \int_{V_1}^{V_f} B_{53}\lambda_\zeta^Y \delta\psi \, dV
\end{aligned}\right\} \quad (A14)$$

where the superscripts on the λ's refer to the final error being solved for. These equations give the terminal values of the variables to be controlled as functions of initial deviations and of the control variables.

Given a desired final value of the state variables to be controlled, there are any number of control variable functions which can be used to attain the desired final values. In particular, there are constant values of the control variables over the interval $V \leq V_1 \leq V_f$ which will result in the desired final values of the controlled state variables. The linearity of the equations allows the addition of the separate conditions to determine the constant values of the control variables that will eliminate off-design conditions in the controlled state variables at the final velocity. The guidance system then calls for control increments which, if held constant, will just eliminate errors in the controlled state variables at the final velocity.

Equations (A14) will be solved for the constant control variables ΔA_T, $\Delta\theta$, and $\Delta\psi$. A shorthand notation will be introduced for the sums and integrals of equations (A14) as follows:

$$E_{SH} = \left[\lambda_h^h \delta h + \lambda_\gamma^h \delta\gamma\right]_{V=V_1}$$

$$E_{SX} = \left[\lambda_h^X \delta h + \delta X + \lambda_\gamma^X \delta\gamma\right]_{V=V_1}$$

$$E_{SY} = \left[\lambda_Y^Y \delta Y + \lambda_\zeta^Y \delta\zeta\right]_{V=V_1}$$

$$I_{TH} = \int_{V_1}^{V_f} \left(B_{11}\lambda_h^h + B_{31}\lambda_\gamma^h\right) dV$$

$$I_{TX} = \int_{V_1}^{V_f} \left(B_{11}\lambda_h^X + B_{21} + B_{31}\lambda_\gamma^X \right) dV$$

$$I_{\theta H} = \int_{V_1}^{V_f} B_{32}\lambda_\gamma^h \, dV$$

$$I_{\theta X} = \int_{V_1}^{V_f} B_{32}\lambda_\gamma^X \, dV$$

$$I_{\psi Y} = \int_{V_1}^{V_f} B_{53}\lambda_\zeta^Y \, dV$$

Equations (A14) may now be written:

$$\left.\begin{aligned} \delta_{hf} &= E_{SH} + \delta A_T I_{TH} + \delta\theta I_{\theta H} \\ \delta X_f &= E_{SX} + \delta A_T I_{TX} + \delta\theta I_{\theta X} \\ \delta Y_f &= E_{SY} + \delta\psi I_{\psi Y} \end{aligned}\right\} \qquad (A15)$$

If δ_{hf} and δY_f are to be zero, equation (A15) must be solved for the control variables:

$$\left.\begin{aligned} \delta A_T &= \frac{(E_{SX} - \delta X_f)I_{TH} - E_{SH}I_{\theta X}}{I_{TH}I_{\theta X} - I_{TX}I_{\theta H}} \\ \delta\theta &= \frac{E_{SH}I_{TX} - (E_{SX} - \delta X_f)I_{TH}}{I_{TH}I_{\theta X} - I_{TX}I_{\theta H}} \\ \delta\psi &= \frac{-E_{SY}}{I_{\psi Y}} \end{aligned}\right\} \qquad (A16)$$

When equations (A16) are expanded and like terms are collected, equations (A16) may be simplified as follows:

$$\left.\begin{aligned} \delta A_T &= \frac{\left[\lambda_h^X I_{\theta H} - \lambda_h^h I_{\theta X}\right]\delta h - I_{\theta H}\delta X_{TG} + \left[\lambda_\gamma^X I_{\theta H} - \lambda_\gamma^h I_{\theta X}\right]\delta\gamma}{I_{TH}I_{\theta X} - I_{TX}I_{\theta H}} \\ \delta\theta &= \frac{\left[\lambda_h^h I_{TX} - \lambda_h^X I_{TH}\right]\delta h + I_{TH}\delta X_{TG} + \left[\lambda_\gamma^h I_{TX} - \lambda_\gamma^X I_{TH}\right]\delta\gamma}{I_{TH}I_{\theta X} - I_{TX}I_{\theta H}} \\ \delta\psi &= -\left[\frac{\lambda_Y^Y \delta Y + \lambda_\zeta^Y \delta\zeta}{I_{\psi Y}}\right] \end{aligned}\right\} \qquad (A17)$$

Equations (A17) will be used to develop the guidance system. In equations (A17) let

$$F_h^{A_T} = \frac{\lambda_h^X I_{\theta H} - \lambda_h^h I_{\theta X}}{D}$$

$$F_X^{A_T} = \frac{-I_{\theta H}}{D}$$

$$F_\gamma^{A_T} = \frac{\lambda_\gamma^X I_{\theta H} - \lambda_\gamma^h I_{\theta X}}{D}$$

$$F_H^\theta = \frac{\lambda_h^h I_{TX} - \lambda_h^X I_{TH}}{D}$$

$$F_X^\theta = \frac{I_{TH}}{D}$$

$$F_\gamma^\theta = \frac{\lambda_\gamma^h I_{TX} - \lambda_\gamma^X I_{TH}}{D}$$

$$F_Y^\psi = \frac{-\lambda_Y^Y}{I_{\psi Y}}$$

$$F_\zeta^\psi = \frac{-\lambda_\zeta^Y}{I_{\psi Y}}$$

where

$$D = I_{TH} I_{\theta X} - I_{TX} I_{\theta H}$$

Substituting in equations (A17) gives:

$$\left.\begin{aligned} \Delta A_T &= F_h^{A_T}\delta h + F_X^{A_T}\delta X_{TG} + F_\gamma^{A_T}\delta\gamma \\ \Delta\theta &= F_h^\theta \delta h + F_X^\theta \delta X_{TG} + F_\gamma^\theta \delta\gamma \\ \Delta &= F_Y^\psi \delta Y + F_\zeta^\psi \delta\zeta \end{aligned}\right\} \qquad \text{(A18)}$$

These equations are used to compute control variable corrections and, when added to reference trajectory values of the control variables, give the following control equations:

$$\left.\begin{aligned} A_T(V) &= A_{Tr}(V) + F_h^{A_T}(V)\delta h + F_X^{A_T}(V)\delta X_{TG} + F_\gamma^{A_T}(V)\delta\gamma \\ \theta(V) &= \theta_r(V) + F_h^{\theta}(V)\delta h + F_X^{\theta}(V)\delta X_{TG} + F_\gamma^{\theta}(V)\delta\gamma \\ \psi(V) &= \psi_r(V) + F_Y^{\psi}(V)\delta Y + F_\zeta^{\psi}(V)\delta\zeta \end{aligned}\right\} \qquad \text{(A19)}$$

These are the specific control equations used in this investigation.

REFERENCES

1. Lessing, Henry C.; Tunnell, Phillips J.; and Coate, Robert E.: Lunar Landing and Long-Range Earth Reentry Guidance by Application of Perturbation Theory. AIAA J. Spacecraft and Rockets, vol. 1, no. 2, March-April, 1964, pp. 191-196.

2. Queijo, M. J.; and Miller, G. Kimball, Jr.: Analysis of Two Thrusting Techniques for Soft Lunar Landings Starting From a 50-Mile Altitude Circular Orbit. NASA TN D-1230, 1962.

3. Citron, S. J.; Dunin, S. E.; and Meissinger, H. F.: A Self-Contained Terminal Guidance Technique for Lunar Landing. ARS Paper 2685-62.

4. Kriegsman, Bernard A.; and Reiss, Martin H.: Terminal Guidance and Control Techniques for Soft Lunar Landing. ARS J., vol. 32, no. 3, March 1962.

5. Queijo, M. J.; Miller, G. Kimball, Jr.; and Fletcher, Herman S.: Fixed-Base-Simulator Study of the Ability of a Pilot to Perform Soft Lunar Landings. NASA TN D-1484, 1962.

6. Barker, L. Keith; and Queijo, M. J.: A Technique for Thrust-Vector Orientation During Manual Control of Lunar Landings From a Synchronous Orbit. NASA TN D-2298, 1964.

7. Sivo, J. N.; and Campbell, C. E.: Analog Study of Descents From Lunar Orbit. NASA TN D-1530, 1962.

8. Tsien, Hsue Shen: Engineering Cybernetics. McGraw-Hill Book Co., Inc., 1954, pp. 178-197.

9. Bliss, Gilbert Ames: Mathematics for Exterior Ballistics. John Wiley and Sons, Inc., N. Y., 1944.

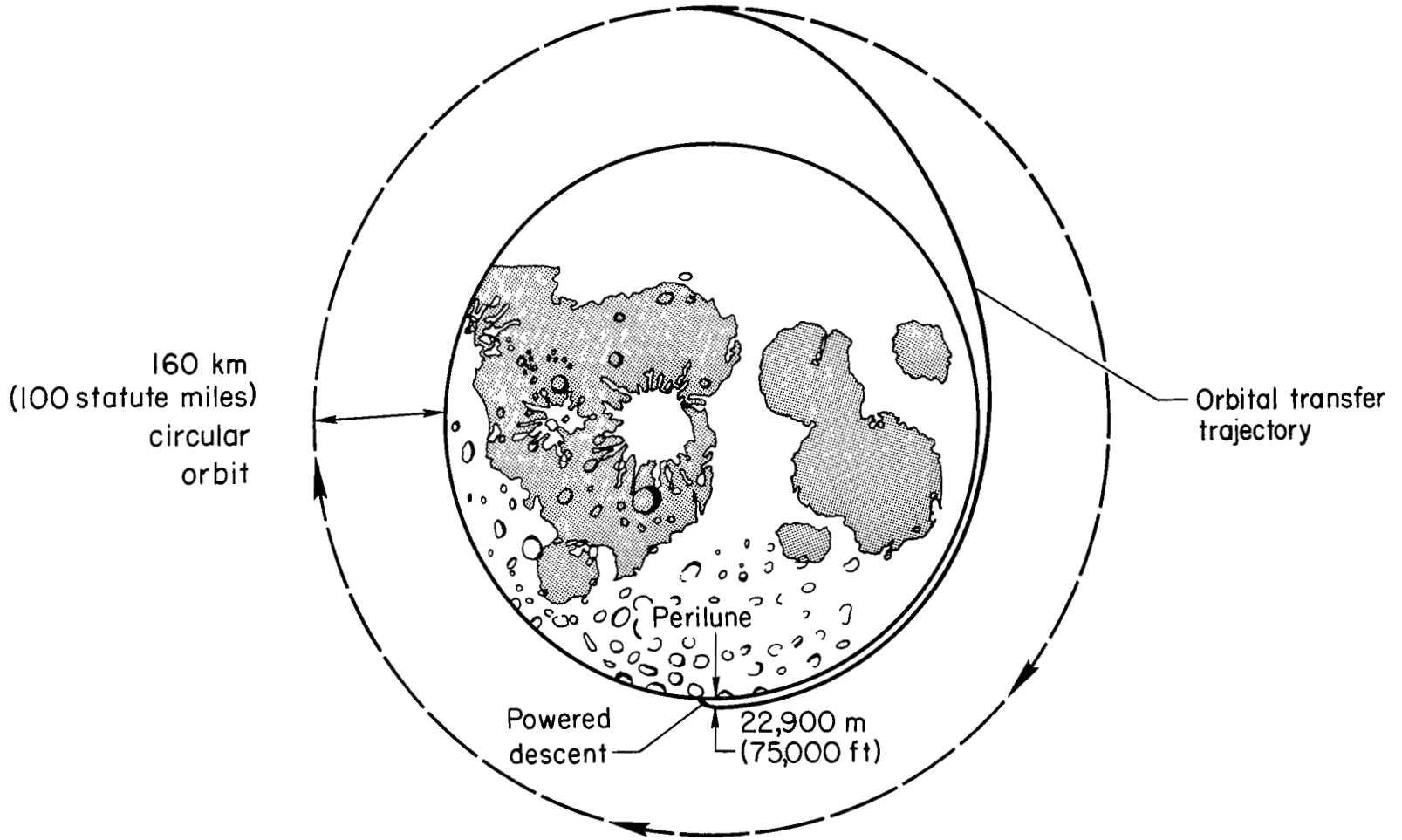

Figure 1.- Lunar landing maneuver.

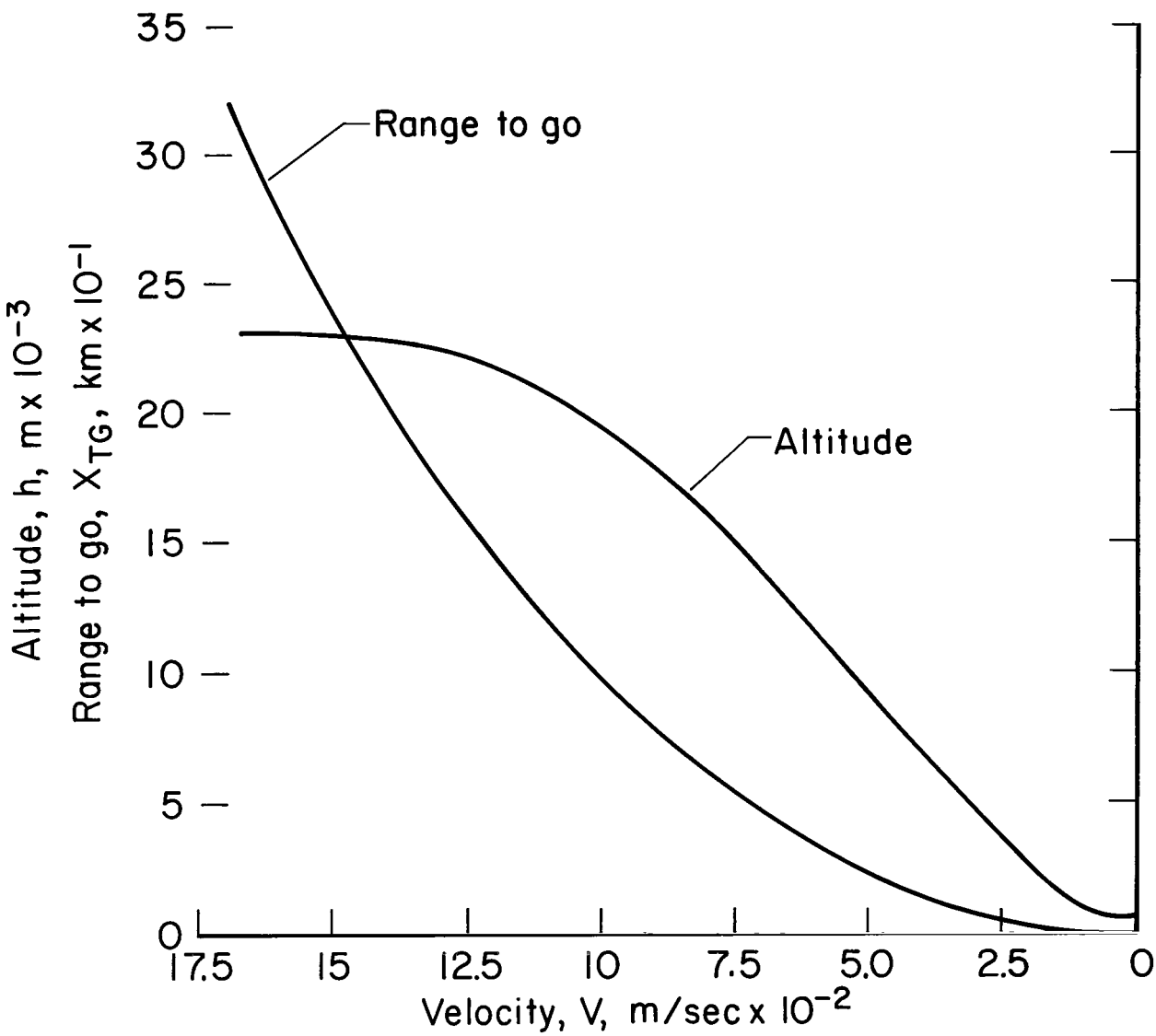

(a) Altitude and range to go.

Figure 2.- Reference trajectory variables.

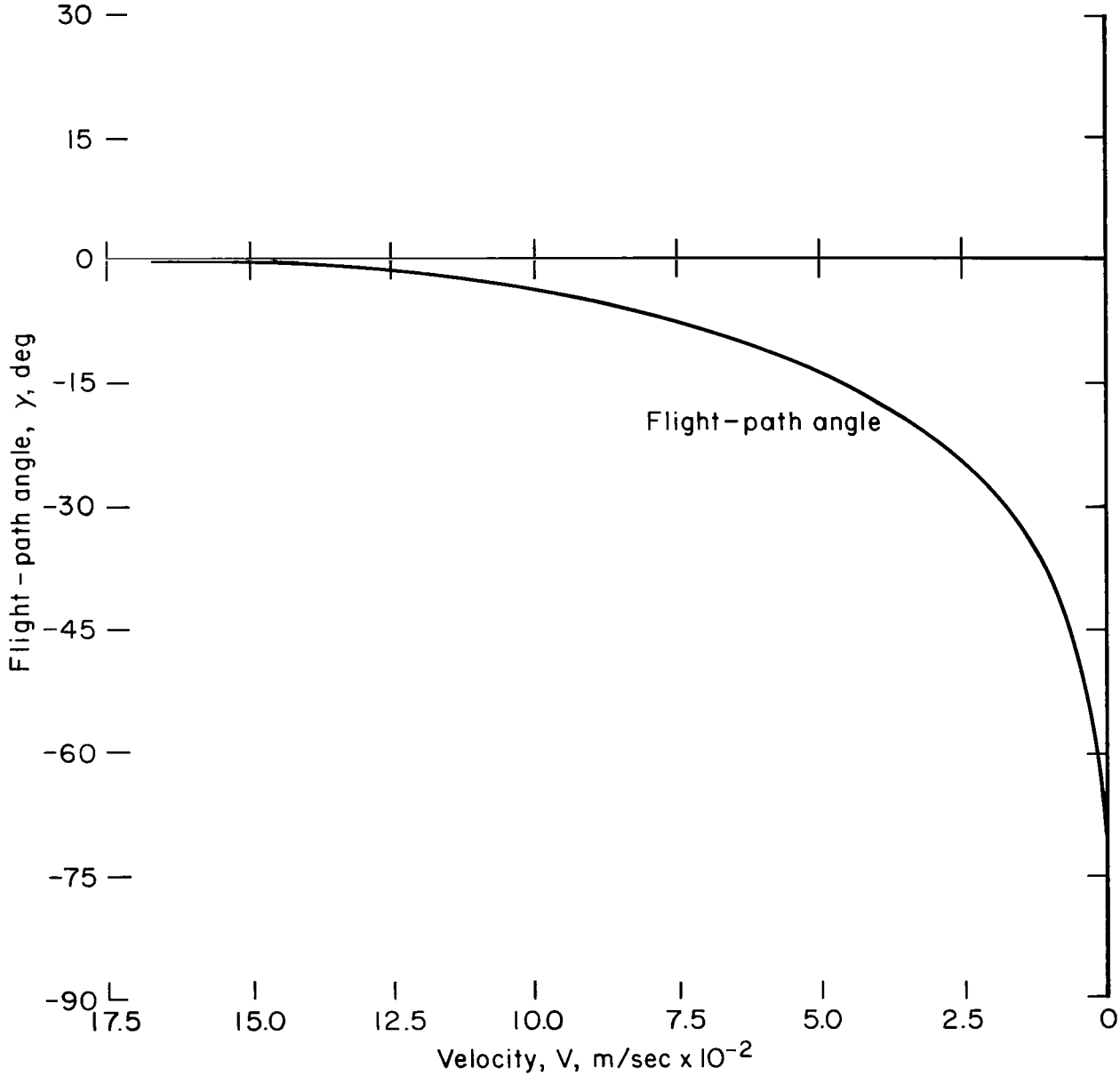

(b) Flight-path angle.

Figure 2.- Continued.

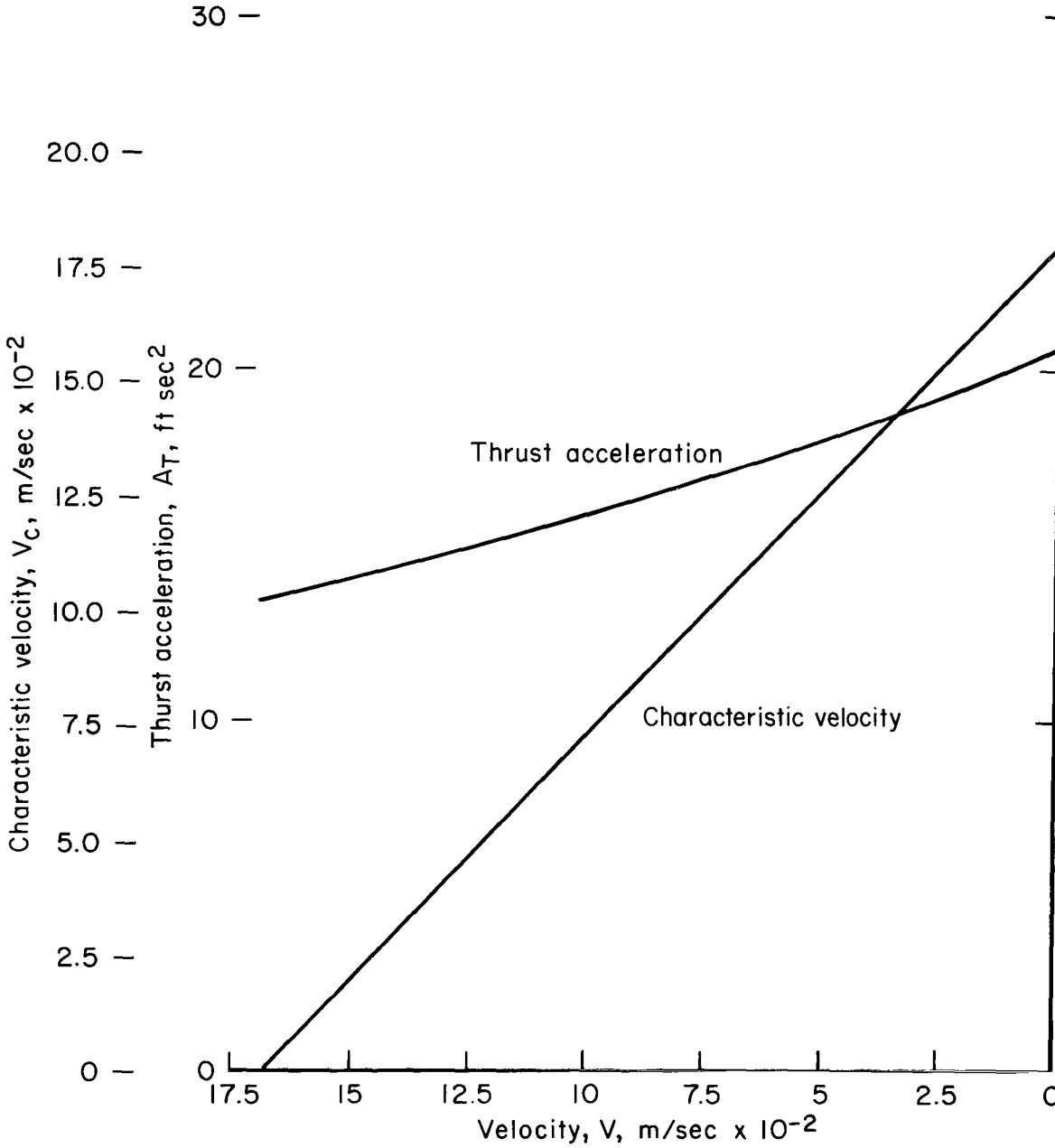

(c) Characteristic velocity and thrust acceleration.

Figure 2.- Concluded.

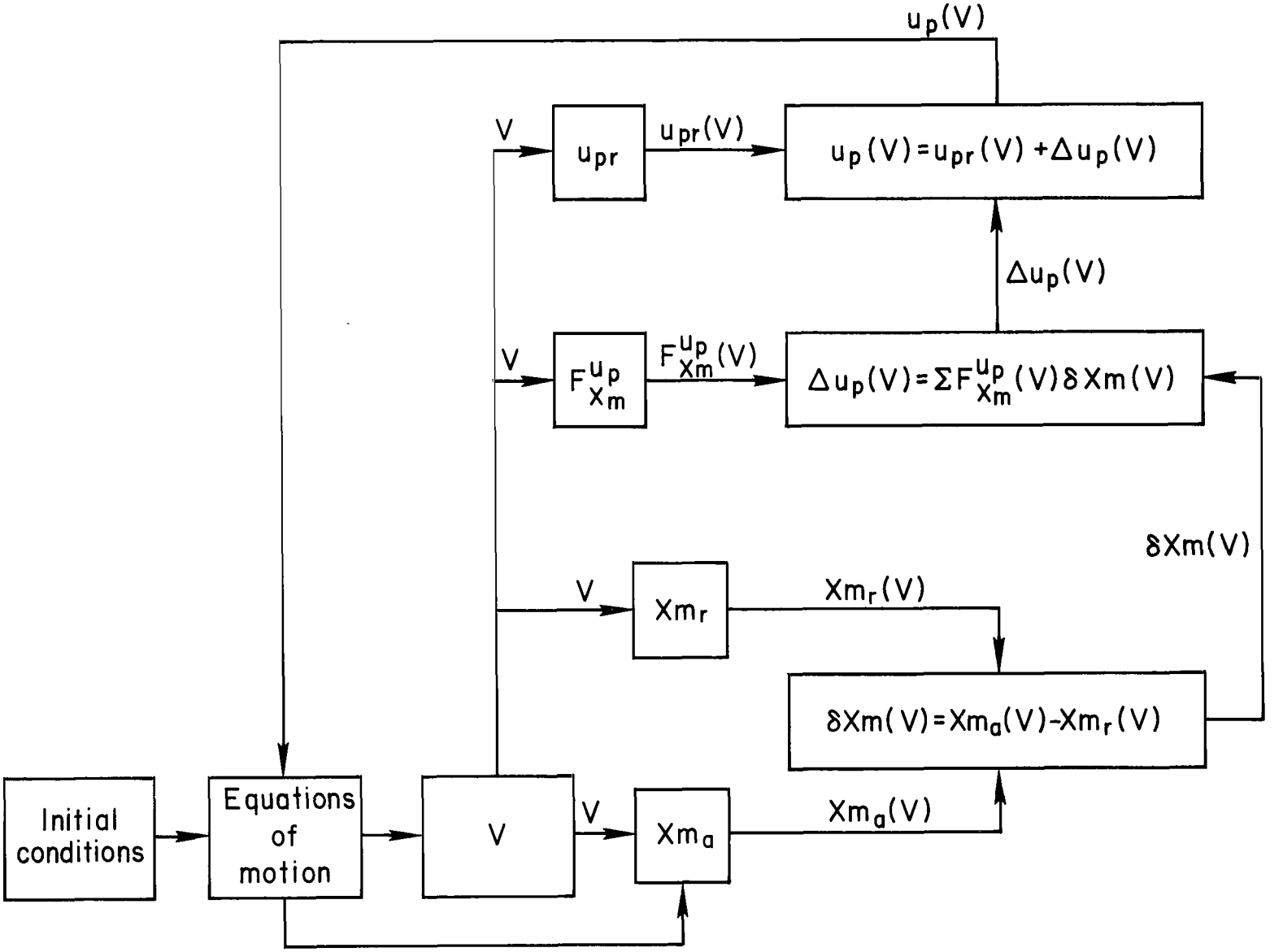

Figure 3.- Terminal control system; where $U_p = A_T, \theta, \psi$; $X_m = h, X, \gamma, Y, \zeta$.

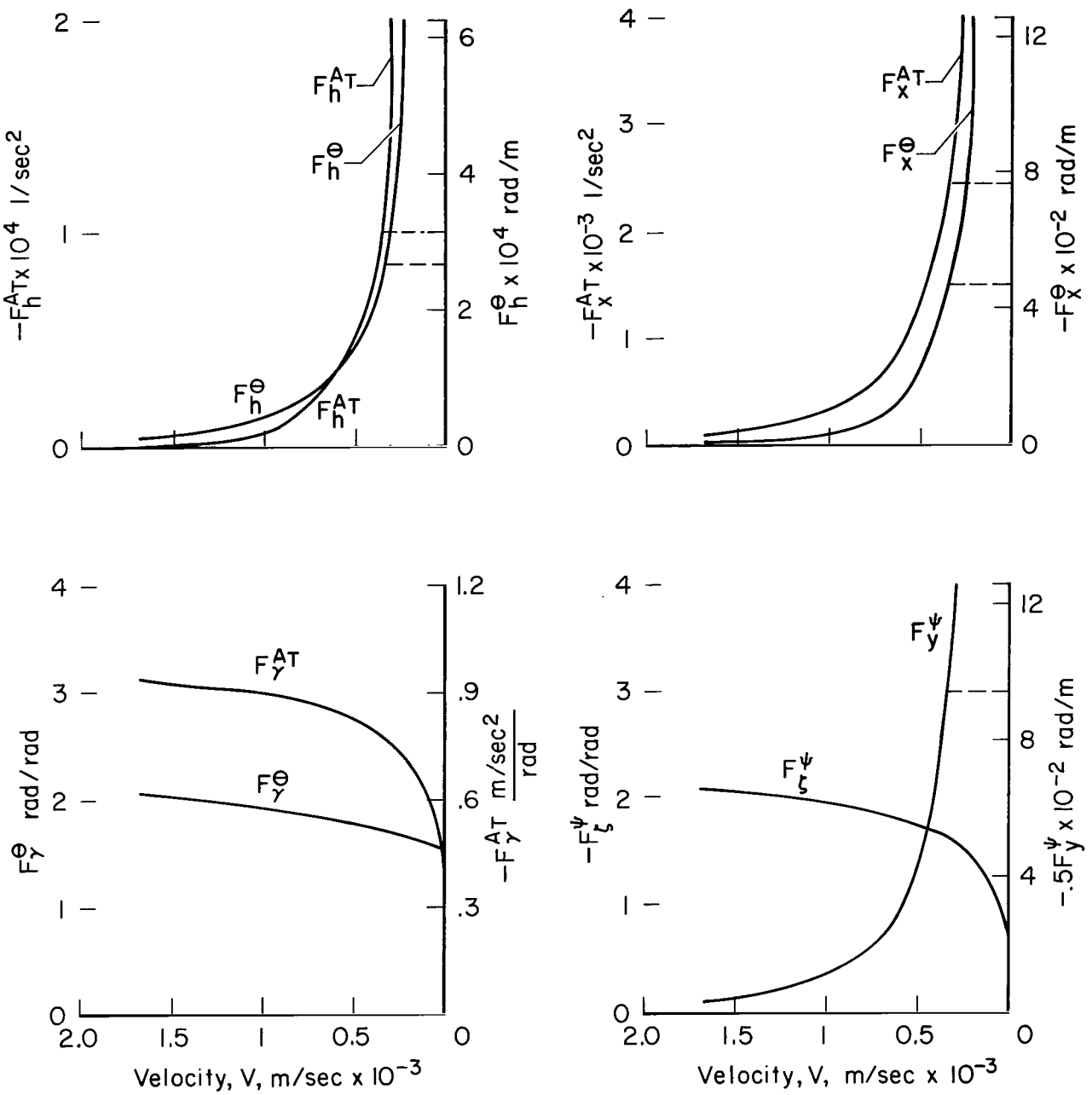

Figure 4.- Linear theory guidance gains.

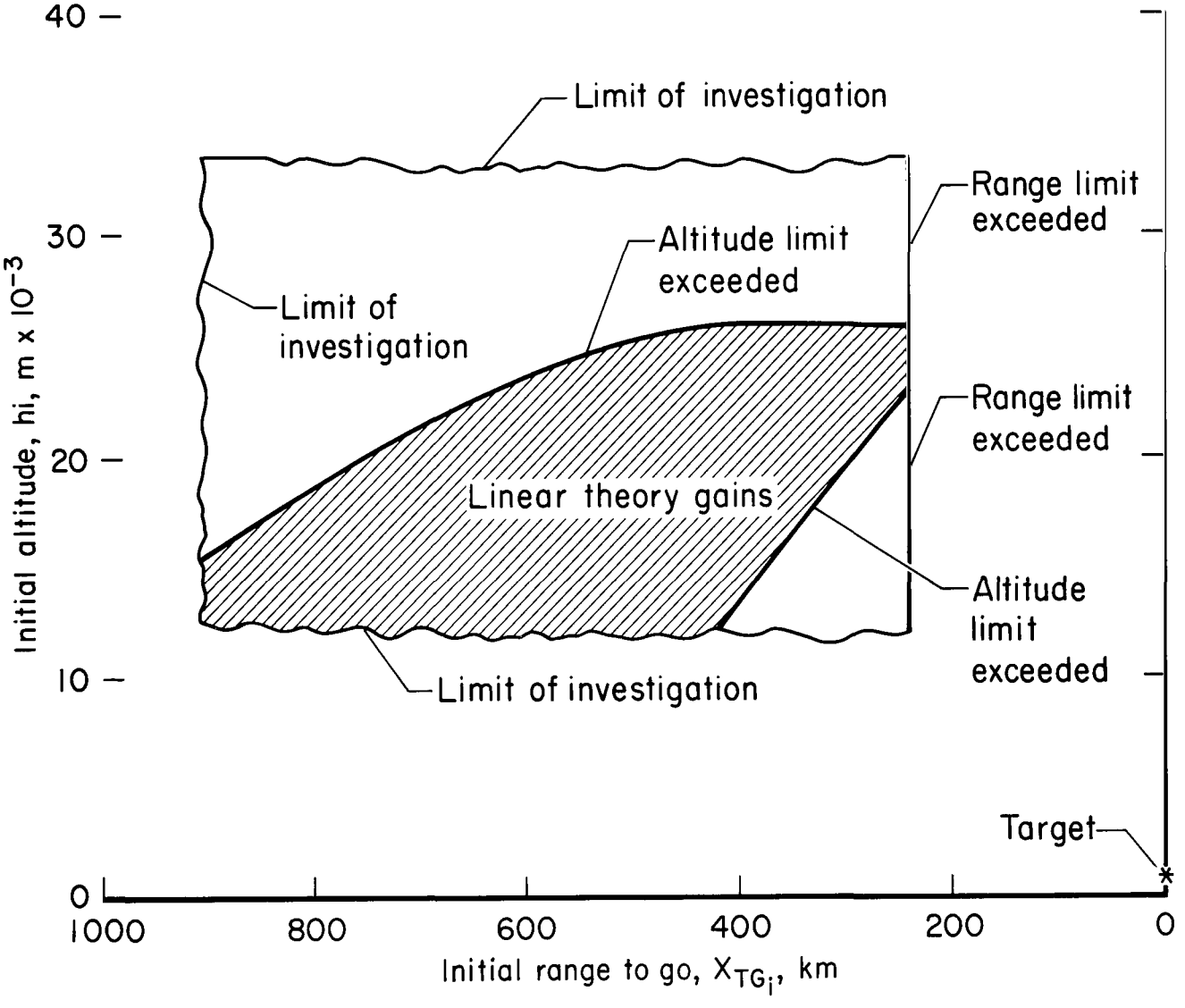

(a) Descent initiated at perilune.

Figure 5.- Guidance capability.

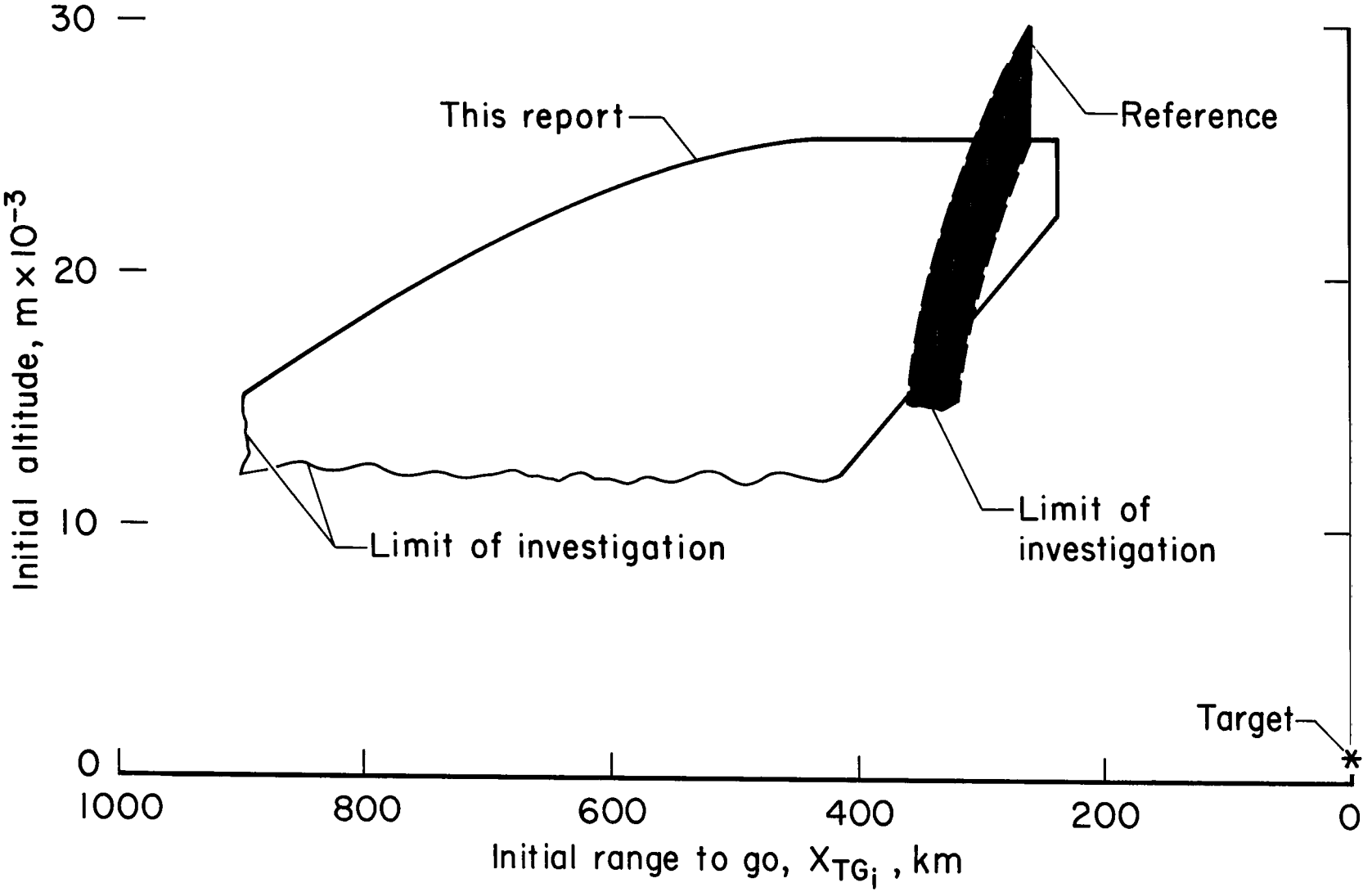

(b) Comparison of guidance capability based on linear theory gains.

Figure 5.- Continued.

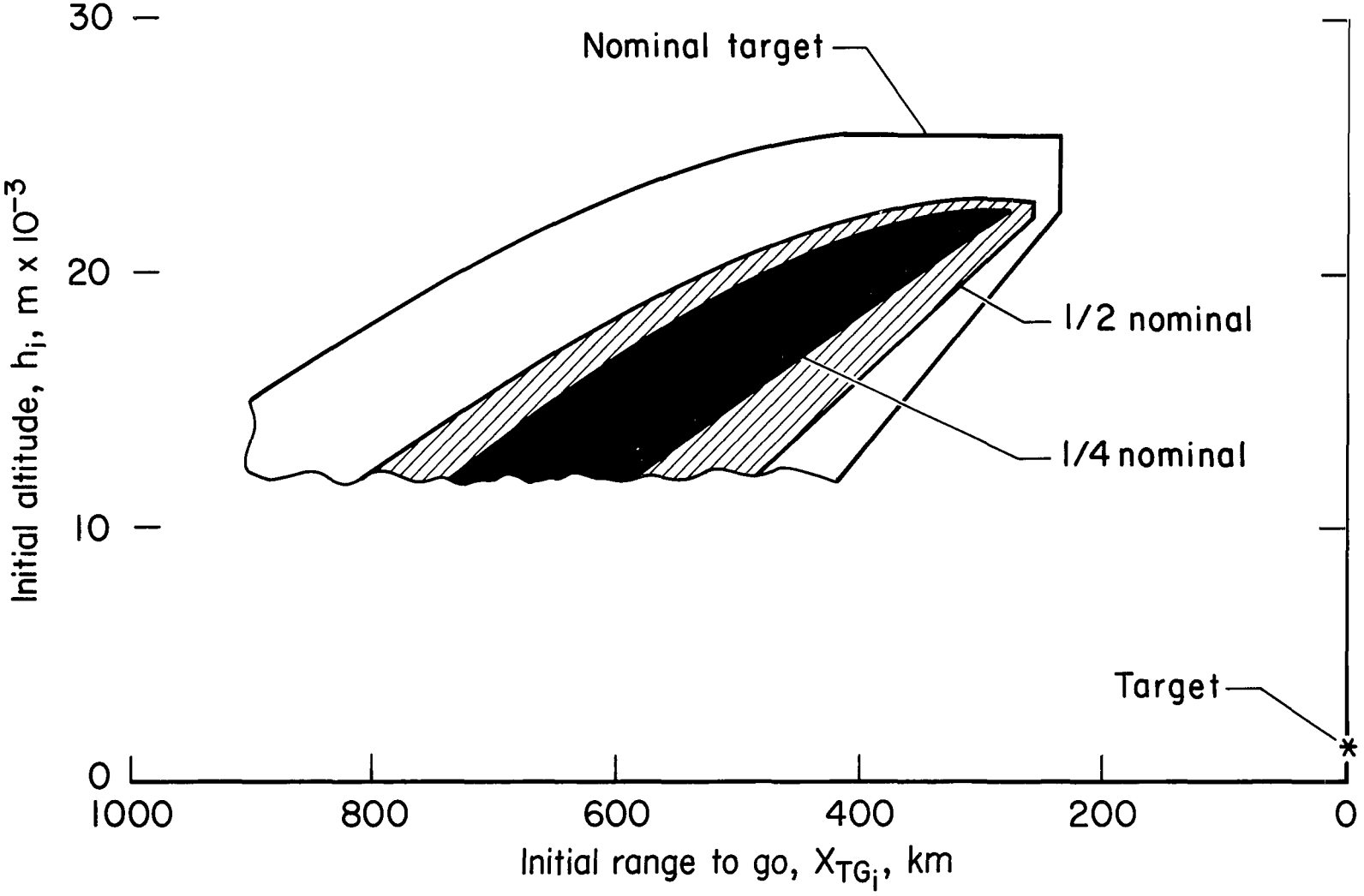

(c) Comparison of linear theory capability for three different targets.

Figure 5.- Continued.

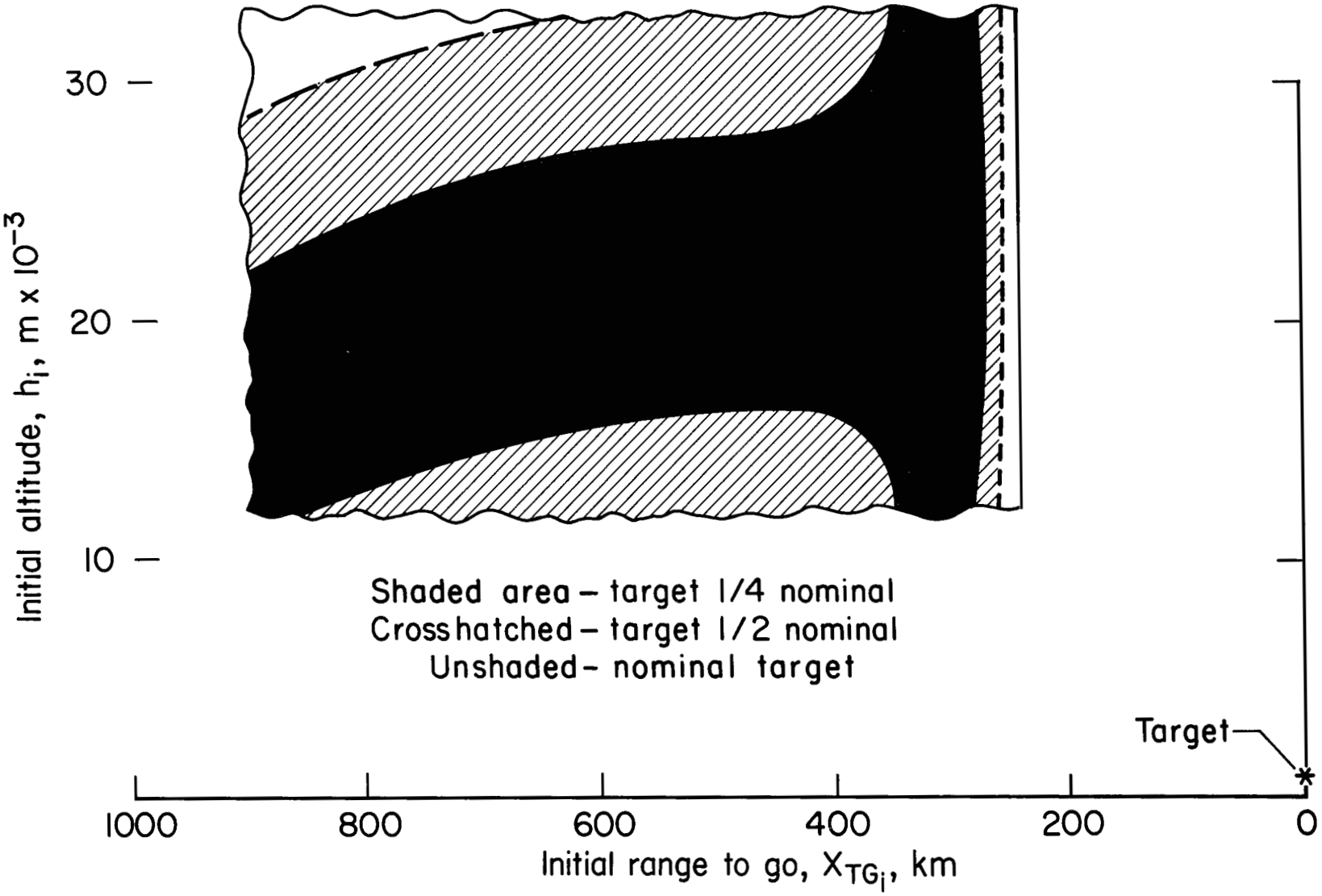

(d) Comparison of guidance capability using empirically adjusted gains for three different targets.

Figure 5.- Concluded.

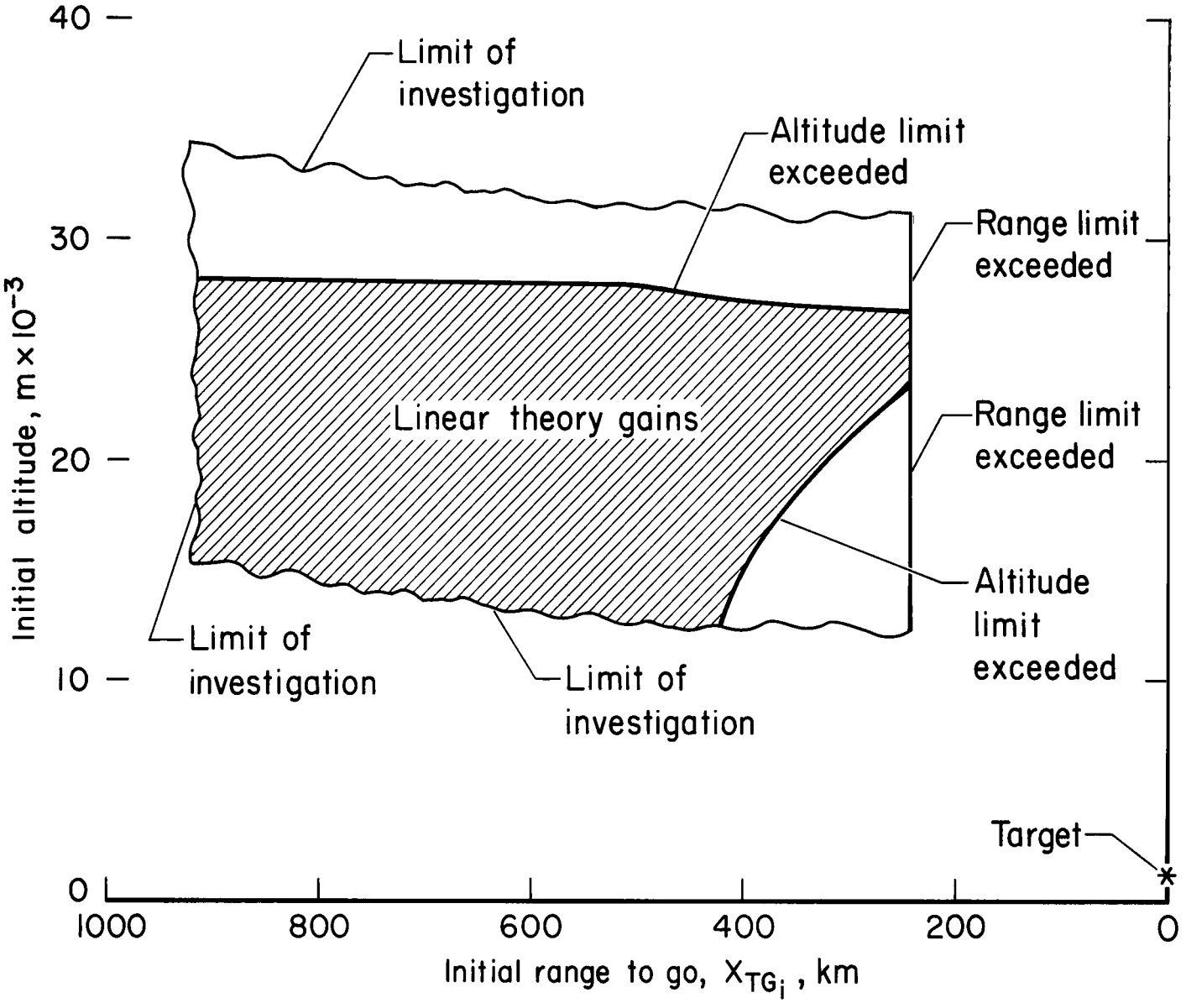

Figure 6.- Guidance capability - descent initiated at point other than perilune.

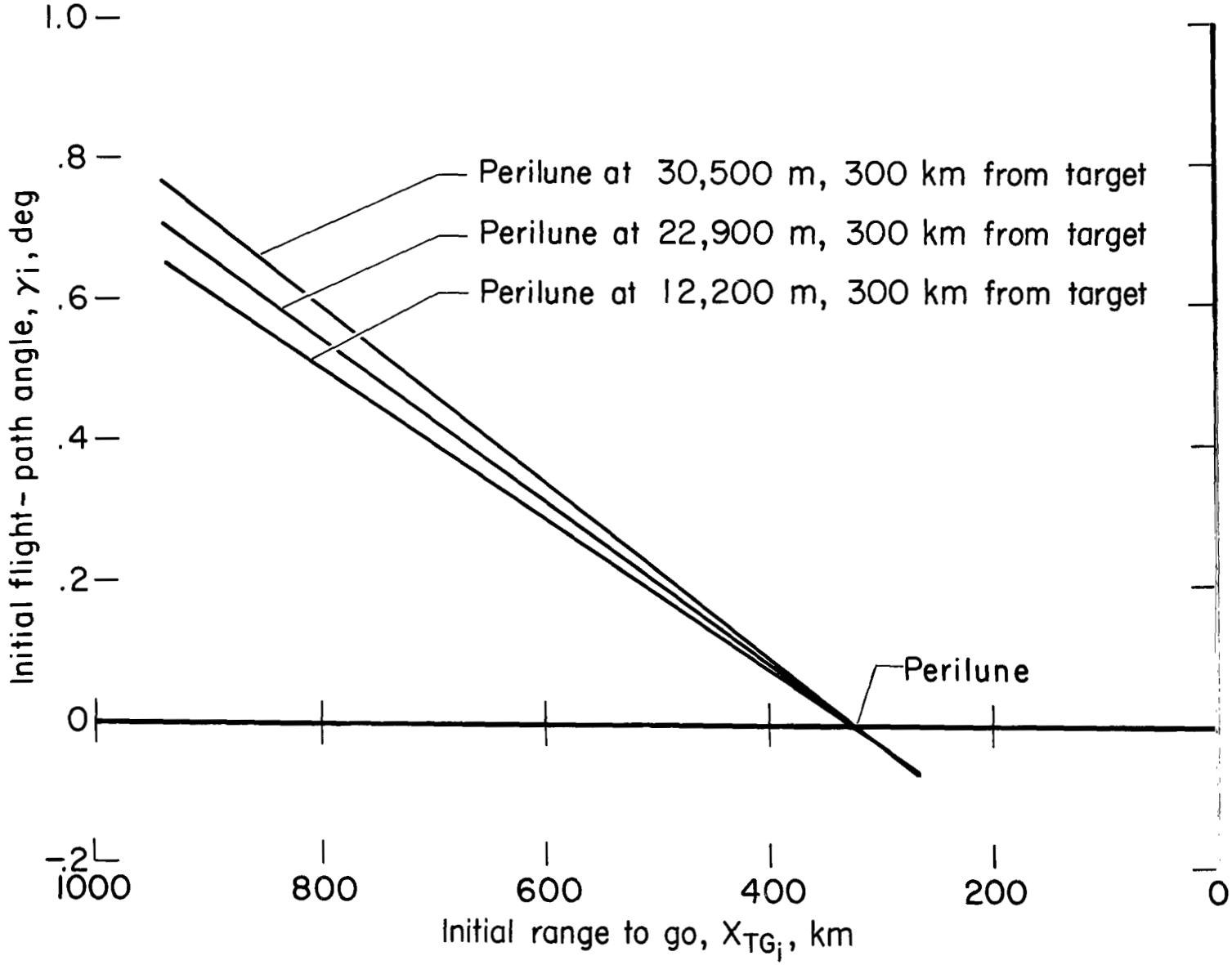

Figure 7.- Initial flight-path angles investigated for data of figure 6.

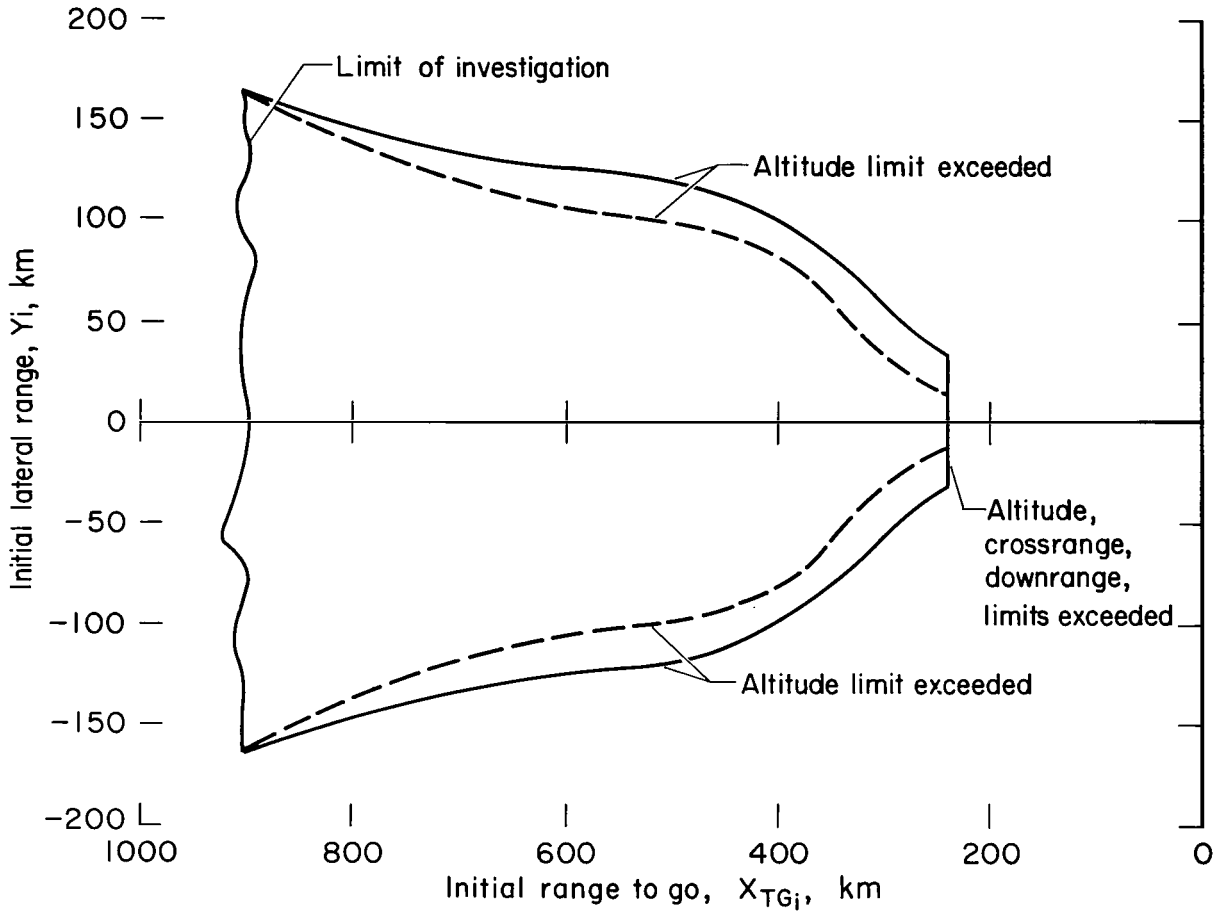

(a) Perilune at 33,500 m (110,000 ft).

Figure 8.- Lateral guidance capability.

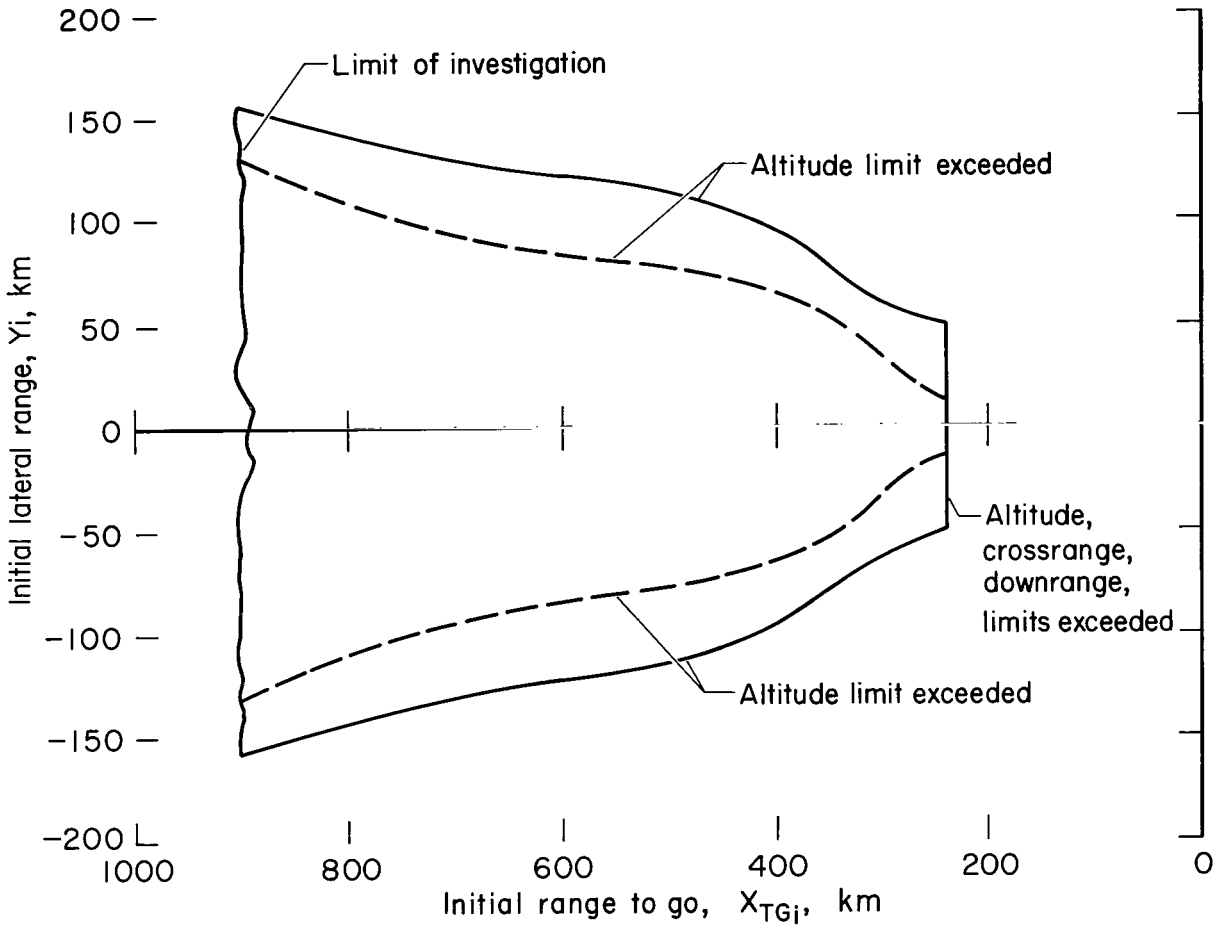

(b) Perilune at 22,900 m (75,000 ft).

Figure 8.- Continued.

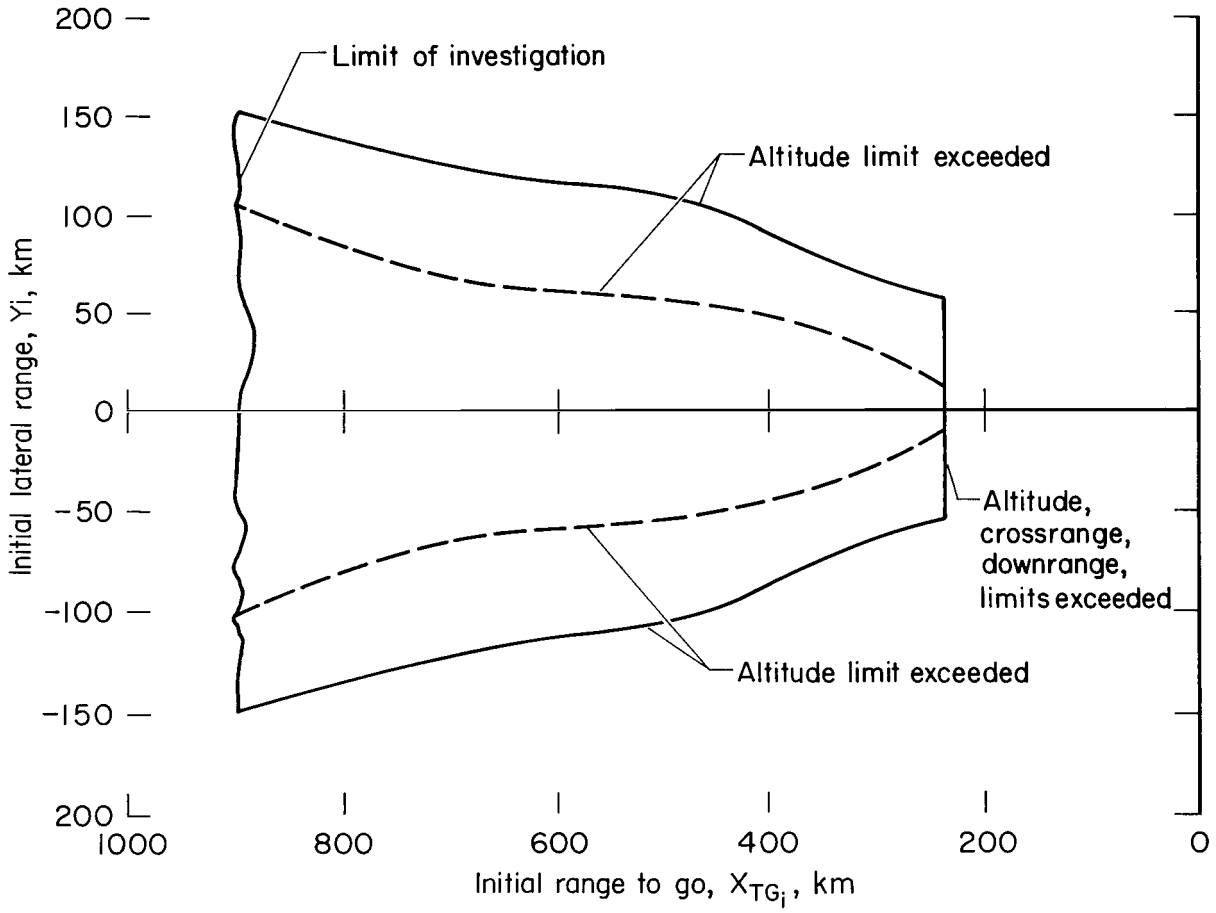

(c) Perilune at 12,200 m (40,000 ft).

Figure 8.- Concluded.

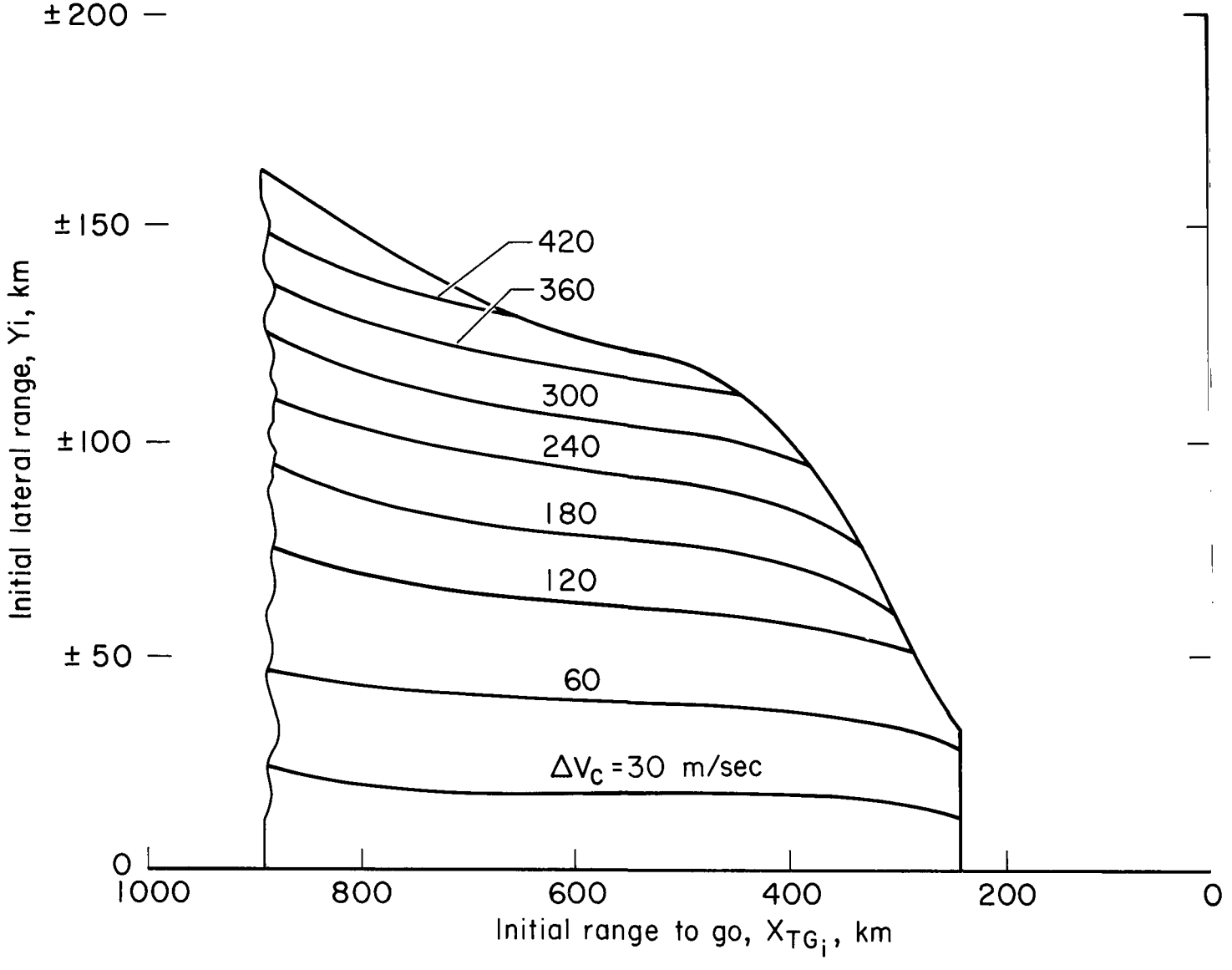

(a) Perilune at 33,500 m (110,000 ft).

Figure 9.- ΔV_c required as function of initial lateral range and initial range to go.

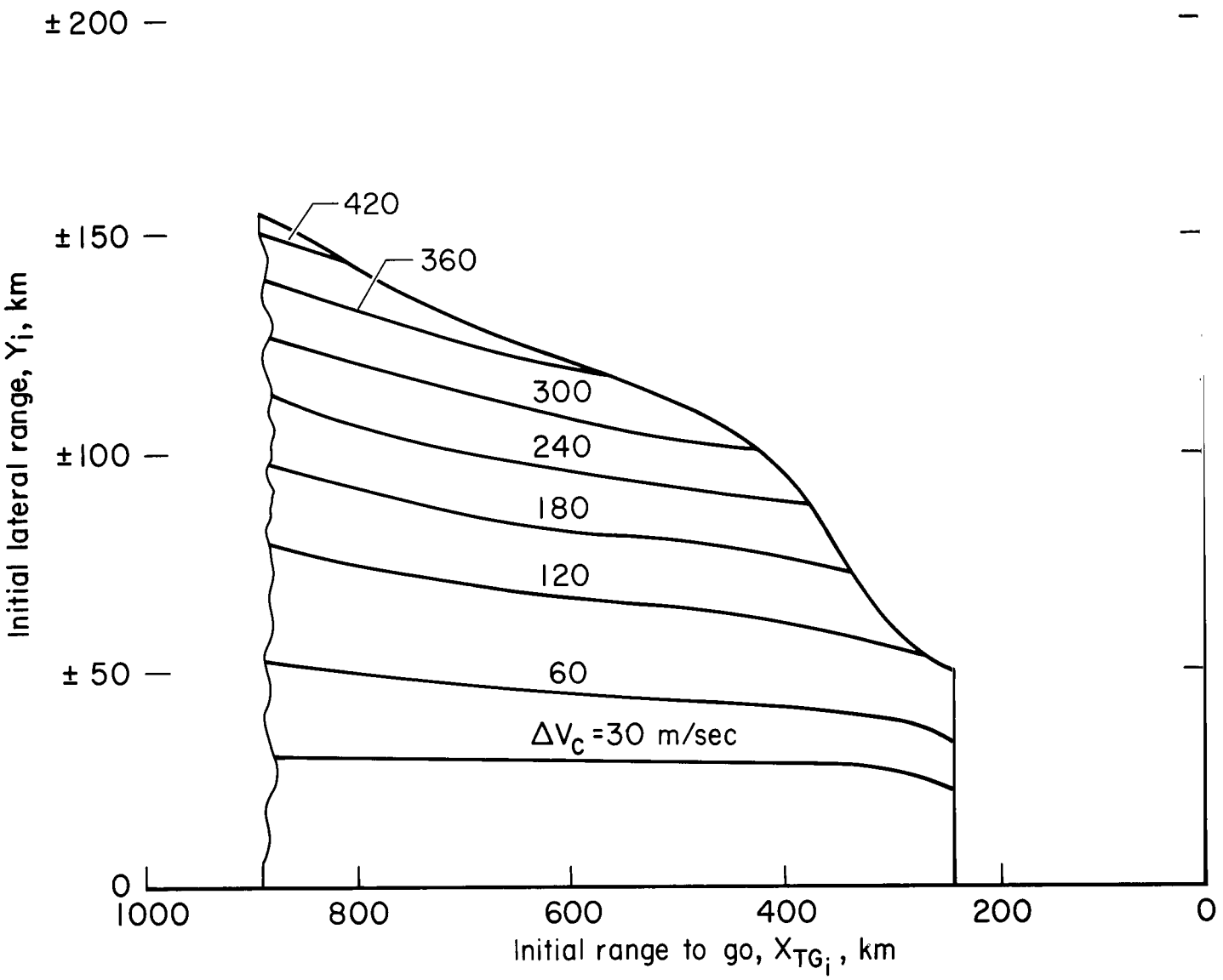

(b) Perilune at 22,900 m (75,000 ft).

Figure 9.- Continued.

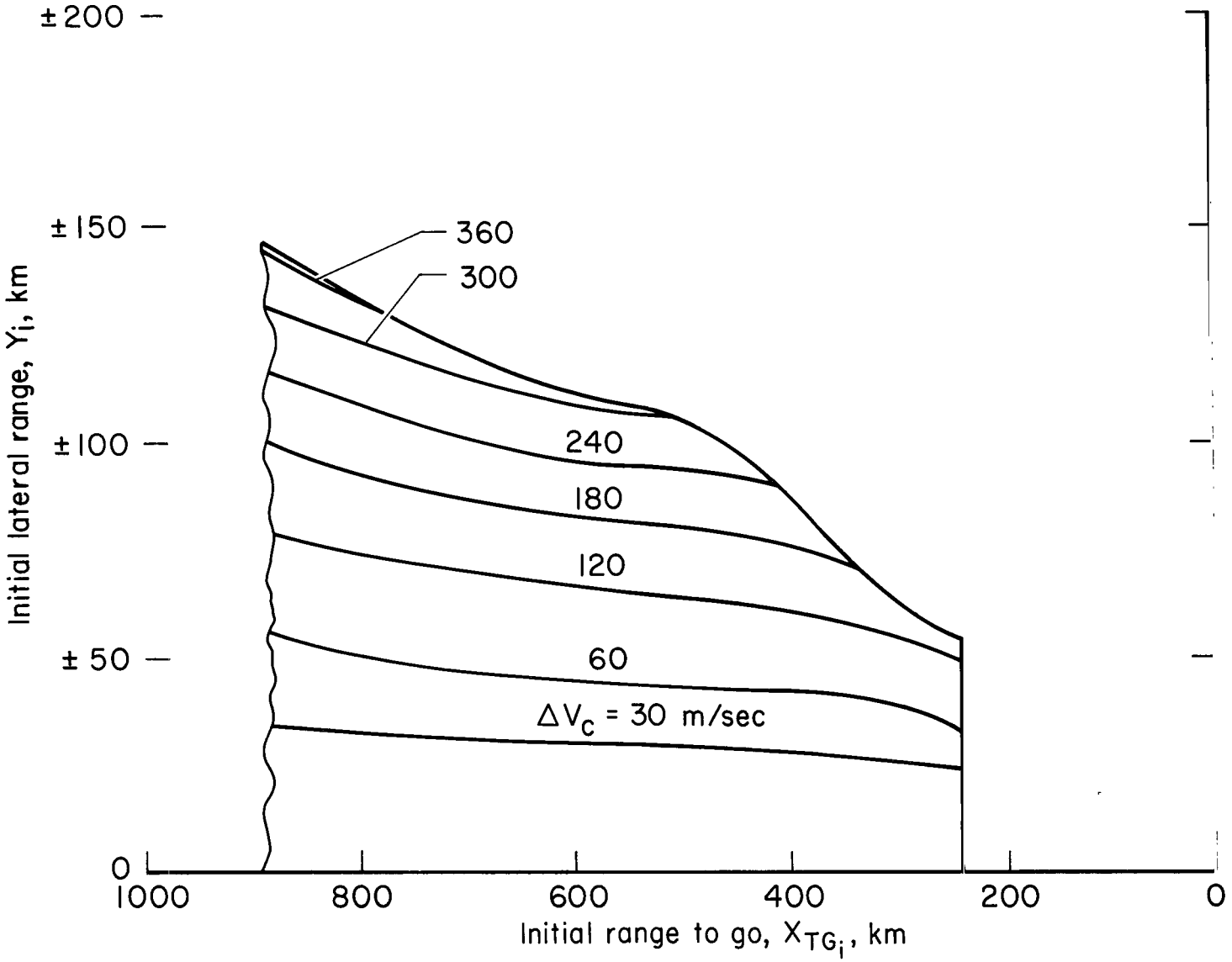

(c) Perilune at 12,200 m (40,000 ft).

Figure 9.- Concluded.

"The aeronautical and space activities of the United States shall be conducted so as to contribute . . . to the expansion of human knowledge of phenomena in the atmosphere and space. The Administration shall provide for the widest practicable and appropriate dissemination of information concerning its activities and the results thereof."

—NATIONAL AERONAUTICS AND SPACE ACT OF 1958

NASA SCIENTIFIC AND TECHNICAL PUBLICATIONS

TECHNICAL REPORTS: Scientific and technical information considered important, complete, and a lasting contribution to existing knowledge.

TECHNICAL NOTES: Information less broad in scope but nevertheless of importance as a contribution to existing knowledge.

TECHNICAL MEMORANDUMS: Information receiving limited distribution because of preliminary data, security classification, or other reasons.

CONTRACTOR REPORTS: Technical information generated in connection with a NASA contract or grant and released under NASA auspices.

TECHNICAL TRANSLATIONS: Information published in a foreign language considered to merit NASA distribution in English.

TECHNICAL REPRINTS: Information derived from NASA activities and initially published in the form of journal articles.

SPECIAL PUBLICATIONS: Information derived from or of value to NASA activities but not necessarily reporting the results of individual NASA-programmed scientific efforts. Publications include conference proceedings, monographs, data compilations, handbooks, sourcebooks, and special bibliographies.

Details on the availability of these publications may be obtained from:

SCIENTIFIC AND TECHNICAL INFORMATION DIVISION

NATIONAL AERONAUTICS AND SPACE ADMINISTRATION

Washington, D.C. 20546